The Islamic University of Gaza

Deanery of Graduate Studies

Faculty of Engineering

Electrical Engineering Department

FUZZY CONTROL STRATEGY FOR THE LOW BANDWIDTH ACTIVE SUSPENSION SYSTEM

By

Mohammed Hafez F. AbuShaban

Advisors

Dr. Mahir B. Sabra

Dr. Iyad A. Abuhadrous

A Thesis Submitted in Partial Fulfillment of the Requirements for the Degree of Master of Science in Electrical Engineering/ Control Systems

1433 هـ – 2012 م

بسم الله الرحمن الرحيم

الجامعة الإسلامية – غزة
The Islamic University - Gaza

عمادة الدراسات العليا هاتف داخلي: 1150

الرقم Ref ...ج س غ/35/...

التاريخ Date ...2012/06/11م...

نتيجة الحكم على أطروحة ماجستير

بناء على موافقة عمادة الدراسات العليا بالجامعة الإسلامية بغزة على تشكيل لجنة الحكم على أطروحة الباحث/ **محمد حافظ فهمي أبو شعبان** لنيل درجة الماجستير في **كلية *الهندسة*** قسم **الهندسة الكهربائية-أنظمة التحكم** وموضوعها:

Fuzzy control strategy for low bandwidth active suspension system

وبعد المناقشة العلنية التي تمت اليوم الاثنين 21 رجب 1433هـ، الموافق 2012/06/11م الساعة الحادية عشرة صباحًا بمبنى القدس، اجتمعت لجنة الحكم على الأطروحة والمكونة من:

د. ماهر بدر صبرة	مشرفاً ورئيساً	.....
د. إياد محمدأيوب أبو هدروس	مشرفًا	.....
د. حاتم علي العايدي	مناقشاً داخلياً	.....
د. باسل محمود حمد	مناقشًا داخليًا	.....

وبعد المداولة أوصت اللجنة بمنح الباحث درجة الماجستير في **كلية *الهندسة*/ قسم الهندسة الكهربائية- أنظمة التحكم.**

واللجنة إذ تمنحه هذه الدرجة فإنها توصيه بتقوى الله ولزوم طاعته وأن يسخر علمه في خدمة دينه ووطنه.

والله ولي التوفيق،،،

عميد الدراسات العليا

أ.د. فؤاد علي العاجز

P.O. Box 108, Rimal, Gaza, Palestine fax: +970 (8) 286 0800 فاكس Tel: +970 (8) 286 0700 ص.ب 108 الرمال، غزة، فلسطين هاتف
public@iugaza.edu.ps www.iugaza.edu.ps

ABSTRACT

In this study, we propose new control strategies for the control of an electro-hydraulically controlled active suspension system. A PID, along with fuzzy control is employed to form a switch between bump isolation and inertial load rejection strategies. Also, PID and optimized PID control are applied for different control approaches throughout this study. Our study propose a special construction of the suspension system where the electro-hydraulic actuator is to be placed in series with the conventional passive one to form a special case of low frequency active suspensions. The full dynamics of the electro-hydraulic servo valve and hydraulic actuator are employed. The proposed control strategies are applied to a quarter car model. Response of the three proposed control strategies is tested for different road profiles and riding conditions including car chassis rolling effect when cornering and pitch movements when braking/ accelerating. Results show superior performance of our modified controllers, especially the optimized PID approach, over passive suspensions and many other controllers of previous studies. Simulations of the optimized PID approach show that our proposed controller provides better passenger comfort as it lowers maximum body acceleration by 94.3% and with reduction in body travel by 98.8% of that of passive one. The three proposed control strategies also show better road handling and car stability over a whole range of road and inertial disturbances.

Control strategies introduced in this study are also applied to a half-car model to test mutual reactions between front and rear sides of the vehicle and our control strategies show superior performance in ride quality over passive suspension.

المُلَخَّص

"استراتيجيةُ تحكمٍ ضبابيّ للتحكمِ في أنظمة التعليق الفعّالة منخفضةِ التردُّد "

في هذه الدراسةِ، نقترحُ إستراتيجيةَ تحكمٍ لنظامِ التعليقِ الفعّالِ المُقادِ كَهروهَيدروليكياً. يتمُّ توظيفُ التحكمِ التناسُبيِّ- التكامُليِّ- التفاضُليِّ مَعَ التحكمِ الضبابيِّ لتكوينِ مُبدِّلٍ بينَ إستراتيجيتيِّ تحكمٍ: عَزلُ المطبّاتِ، و ممانعةُ الحِملِ الناتجِ عنِ القصورِ الذاتيِّ لكتلةِ المركبةِ. كذلكَ، يتمُّ استخدامُ حاكمٍ تناسُبيِّ- تكامُليِّ- تفاضُليِّ مُنغَّمٍ بطريقةِ أمثليّةٍ لتحقيقِ طريقةِ تحكمٍ أخرى تُعرضُ خلالَ هذه الدراسةِ. الدراسةُ تقترحُ تركيباً خاصاً لنظامِ التعليقِ حيثُ يتمُّ وضعُ المشغِّلِ الكَهروهَيدروليكيِّ على التوالِي معَ نظامِ التعليقِ التقليديِّ ليُشكِّلَ حالةً خاصةً من نُظُمِ التعليقِ الفعّالةِ منخفِضةِ التردّدِ. يتمُّ احتسابُ كافةِ الخواصِّ الديناميكيةِ للصمامِ الكَهروهَيدروليكيِّ المؤازِرِ بالإضافةِ للمُشَغِّلِ الهيدروليكيِّ المستخدَمِ. يتمُّ تطبيقُ استراتيجياتِ التحكمِ على نموذجِ رُبُعِ مَركبةٍ و يتمُّ فحصُ استجابةِ إستراتيجياتِ التحكمِ المقترحةِ على طُرُقٍ و ظروفِ قيادةٍ مختلفةٍ بما في ذلكَ تأثيرُ المَيْلِ الجانبيِّ لجسمِ المَركبةِ أثناءَ الانعطافِ، و مَيْلُ الجسمِ للأمامِ و الخلفِ في حالاتِ التوقُّفِ و التسارعِ. تظهر النتائجُ أداءً متميزاً لأنظمةِ التحكمِ المحسَّنةِ المقترَحةِ، خاصّةً للتحكمِ المنغّمِ بطريقة أمثلية، مقارنةً بنظامِ التعليقِ التقليديّ و العديدِ من الحاكماتِ المقترحةِ في دراساتٍ سابقةٍ. نتائجُ المحاكاةِ تظهرُ أنَّ نظامَنا المقترحُ المنغّم بطريقةٍ أمثلية يقدِّمُ تحسيناً في راحةِ رُكّابِ المركبةِ حيثُ أنّه يقلِّلُ أقصى تسارعٍ رأسيٍّ لجسمِ المركبةِ بنسبةٍ تصلُ إلى ٩٤.٣%، و يقلِّلُ أقصى إزاحةٍ رأسيةٍ لجسمِ المركبةِ بنسبةٍ تصلُ إلى ٩٨.٨% مقارنةً بنظامِ التعليقِ التقليديِّ. بالإضافةِ لذلكَ، يظهرُ نظامُنا المقترَحُ تحسيناً على صعيدِ تماسُكِ المركبةِ و استقرارِها على مجالٍ واسعٍ من التشويشاتِ الناجمةِ عن ظروفِ الطريقِ أو القصورِ الذاتيِّ لكتلةِ المركبةِ.

كذلكَ يتمُّ تطبيقُ إستراتيجياتِ التحكمِ المقدَّمةِ في هذه الدراسةِ على نموذجِ نصفِ مركبةٍ لفحصِ استجابةِ نظامِنا للتأثيراتِ المتبادَلةِ بينَ طرَفَيِّ المركبةِ الأماميِّ و الخلفيِّ، و يُظهِرُ نظامُنا أداءً متميزاً في جودةِ القيادةِ مقارنةً بالنظامِ التقليديّ.

DEDICATION

To my beloved parents, my wife, and my kids.

ACKNOWLEDGMENT

No words can express my deep thanks to my parents and my wife for their patience and constant encouragement and support throughout my work.

I'd like to thank my thesis advisors, Dr. Mahir Sabra and Dr. Iyad Abuhadrous, for their guidance and helpful notes throughout this work. Many thanks and appreciations to my friends, colleagues, and family for their support.

TABLE OF CONTENTS

LIST OF TABLES

LIST OF FIGURES

LIST OF SYMBOLS

Symbol	Description
Quarter-car model	
m_c	Car body mass [kg]
m_s	Sprung (disc) mass [kg]
m_{us}	Unsprung (wheel) mass [kg]
c_2	Stiffness of spring [N/m]
b	Stiffness of damper [Ns/m]
c_1	Stiffness of pneumatic compressed tire [N/m]
u	Road disturbance [m]
x_{us}	Unsprung mass, wheel, travel [m]
x_s	Sprung mass, disc, travel [m]
x_c	Car body travel [m]
x_s-x_{us}	Suspension deflection [m]
F_{sv}	Force generated by hydraulic actuator [N]
A	Cross sectional area of hydraulic cylinder piston [m^2]
P_L	Pressure drop across cylinder piston [Pa]
V_t	Total actuator volume [m^3]
β_e	Effective bulk modulus [Pa]
Q_L	Hydraulic fluid flow [m^3/s]
C_{tp}	Total leakage coefficient of the piston [m^3/s/Pa]

C_d	Discharge coefficient
w	Spool valve area gradient [m^2/m]
x_v	Displacement of spool valve [m]
ρ	Hydraulic fluid density [kg/m^3]
P_s	Hydraulic supply pressure [Pa]
r	Control signal [Volt or Ampere]
K_{sv}	Scale of servo valve control signal

PID with fuzzy switch control strategy

K_P	Proportional gain for PID with fuzzy switch strategy
K_I	Integral gain for PID with fuzzy switch strategy
K_D	Differentiator gain for PID with fuzzy switch strategy
k_d	Scale of suspension deflection gain
r_1	Control law for bump isolation strategy
r_2	Control law for load rejection strategy
B	Value of first output "Bump" of fuzzy switch
L	Value of second output "Load" of fuzzy switch

PID control schemes, conventional and optimized

K_p	Proportional gain for PID control scheme
K_i	Integral gain for PID control scheme
K_d	Differentiator gain for PID control scheme

Half-car model

m_c	Half-car body mass [kg]
m_f	Front sprung mass, disc [kg]
m_r	Rear sprung mass, disc [kg]
m_{uf}	Front unsprung mass, wheel [kg]
m_{ur}	Rear unsprung mass, wheel [kg]
c_f	Front spring stiffness [N/m]
c_r	Rear spring stiffness [N/m]
b_f	Front damper stiffness [Ns/m]
b_r	Rear damper stiffness [Ns/m]

c_{tf}	Front tire stiffness [Ns/m]
c_{tr}	Rear tire stiffness [Ns/m]
u_f	Front bump disturbance [m]
x_{uf}	Front wheel travel [m]
x_{sf}	Front disc travel [m]
x_f	Body front side travel [m]
u_r	Rear bump disturbance [m]
x_{ur}	Rear wheel travel [m]
x_{sr}	Rear disc travel [m]
x_r	Body rear side travel [m]
F_f	Actuator force for the front side of car body [N]
F_r	Actuator force for the rear side of car body [N]
a	Distance from front axles to car body center of gravity (CG) [m]
b	Distance from rear axles to car body CG [m]
J_y	Moment of inertia of car body [kg.m^2]
θ	Pitch angle of car body [rad]
x	Bounce, vertical travel of body CG [m]

Power and energy

$P(t)$	Instantaneous power need for hydraulic actuator [w]
$F(t)$	Instantaneous force generated across actuator [N]
$v(t)$	Velocity of cylinder piston relative to cylinder body [m/s]
E	Energy consumption [J]

1. INTRODUCTION

1.1. BACKGROUND

Automotive suspensions have a great importance in making ground vehicles more reliable, more comfort, and with less wear due to road roughness. Nowadays, vehicle suspensions are important division of automotive chassis control. Suspensions have a notable improvements in 1960's by applying classical control techniques to passive suspensions. In 1980's, active suspensions were introduced employing electro-hydraulic elements to improve suspension performance.

Automotive active suspensions have attracted interest for research in the few recent decades especially after the large integration in electronic controllers for industrial applications. Also, control engineers have a wide space to contribute in this field by applying modern automatic control schemes with the new developments in active suspension components, i.e., actuators, sensors, precise low-cost electronics and fast microprocessors, [1].

1.2. PASSIVE AND SEMI-ACTIVE SUSPENSIONS

Passive conventional suspensions, shown in Fig. 1.1, contain only passive elements, spring in parallel with a damper, and have good characteristics in achieving passenger comfort and vehicle control, i.e., ride, but not for all road and loading situations. Semi-active suspensions have shown better performance since they have the ability to vary their damping value according to control scheme through using *Electro-Rheological* or *Magneto-Rheological* dampers.

These suspensions need some amount of power to be fed to it. In general, increasing damper stiffness of a suspension gives better handling but with less passenger comfort and vice versa. Usually, suspension design should compromise between these conflicting trade-offs and also is related to cost, [1], [2].

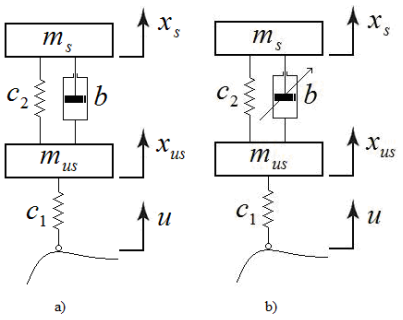

Figure (1.1): Suspensions: a)passive, b) semi-active.

1.3. ACTIVE SUSPENSIONS

Active suspensions have additional hydraulic actuators to the passive elements of conventional ones. These actuators give the suspension the ability to generate needed forces to improve performance characteristics of vehicle ride for all driving situations, [3], [4]. Active suspensions, in addition to their cost, require additional power to be injected to them and this is an important issue to be justified when selecting an active suspension for some vehicle and power consumption of suspension must be taken into consideration, [5].

There are two types of commonly recognized active suspension structures [6], [4], low bandwidth and high bandwidth, as shown in Fig. 1.2. High bandwidth refers to regulation of both the sprung mass of the suspension for vibrations below 3Hz and the unsprung mass, wheel assembly, for vibrations around 12 Hz, [1], [6]. While the low bandwidth suspension regulates only the sprung mass for its low frequency vibrations and the high frequency vibrations are controlled by the passive damper of the system, [6]. Low bandwidth active suspensions have the ability to improve ride comfort but they have limited control on vehicle handling. Whereas high bandwidth ones have the ability to improve both ride comfort and handling but with a penalty of cost increase.

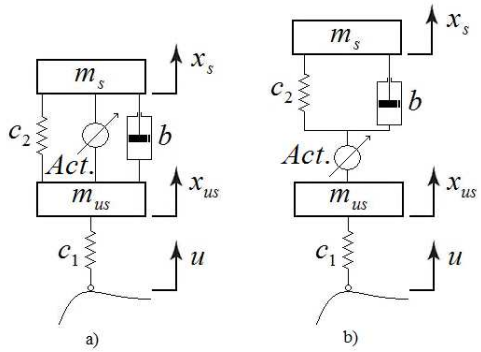

Figure (1.2): Active suspensions: a) high bandwidth (parallel), b) low bandwidth (series).

1.4. PROBLEM STATEMENT

Developments of vehicle suspensions are made to achieve some performance characteristics in order to have a good suspension system. Main characteristics are summarized in [1] to be

a) regulation of body movement: by isolating body from road bumps (passenger comfort) in addition to minimize inertial/ mass transfer disturbances resulting from vehicle cornering (body roll), braking/ acceleration (body pitch), and whole body vertical movement (bounce).

b) regulation of wheel hop: to maintain contact and adhesion between tire and ground (vehicle handling).

c) force distribution: distribution of car weight between the four wheels to get good handling characteristics needs all-time wheel-tire contact.

Different suspension categories, as shown in [2], have been used in commercial vehicles in order to achieve performance characteristics. The Society of Automotive Engineers (SAE) standard regarding human acceptable region and vertical vibration thresholds is cited within [2] and main performance characteristics of a good suspension are regulated in *Ride and vibration data manual* (*SAE J6a*) and *Vehicle dynamics terminology* (*SAE J670e*) standards.

The problem here is to propose and justify a special suspension structure that would give us the ability to use simple linear control techniques instead of nonlinear ones in order to minimize needed computations and be able to control our proposed active suspension with low cost conventional electronic components, e.g. PID controllers.

1.5. RESEARCH OBJECTIVES

Our objectives can be summarized in the following points:

- Propose and justify a special mechanical construction of active suspension.
- Derive mathematical model of our proposed suspension applied to a quarter car suspension model with employing nonlinear dynamics of the hydraulic actuator to be used, then extend the mathematical model to simulate a half-car model.
- Design and develop control strategies that can deal with the nonlinear nature of active suspension, i.e. fuzzy and PID control.
- Visualize system response of our proposed system applied to a quarter-car model.

1.6. THESIS CONTRIBUTION

Main thesis contribution can be summarized in the following points:

- A special low bandwidth active suspension is introduced with full nonlinear dynamics of electro-hydraulic actuator employed.
- New simple control strategies are introduced.
- System and control are tested for different road and inertial disturbances with notable performance improvements.
- System response is visualized in 2D animation.

1.7. THESIS STRUCTURE

The structure of this thesis will be as follows:

In *Chapter* 2 we make our literature review and some historical background of vehicle suspension systems and with emphasis on *active* ones and show previous control schemes. While in *Chapter* 3 we introduce model of proposed suspension structure applied to quarter-car model with employing full dynamics of the hydraulic actuators for simulation purposes. Next in the same chapter, we show proposed suspension control methodologies and then we show how to extend our system and control to a half-car model. Power requirements of active suspensions will be discussed in this chapter as well.

In *Chapter* 4, controlled system simulation and discussion for results obtained are shown for quarter car and half-car models. Comparison between our results and previous studies is demonstrated. Also, power requirements for our proposed control approaches are shown.

Then, in *Chapter* 5, we come to our conclusions and recommendations for future work.

2. LITERATURE REVIEW

2.1. BACKGROUND TO ACTIVE SUSPENSIONS CONTROL

Conventional suspensions are nonlinear due to viscous and coulomb frictions appear in hydraulic dampers. Also, when employing full dynamics of the electro-hydraulic actuators used in high-bandwidth active suspensions, the system becomes highly nonlinear. Thus, nonlinear controllers are more capable to handle high bandwidth active suspensions because they show good capability to switch between operation modes around each equilibrium point of the nonlinear system and adapt to handle all operating conditions. That is, they can improve worst-case road conditions in addition to normal road conditions, [7]. Also, it has been shown that focusing on some specific performance index will lead to limited improvement over passive suspensions, [7]. Thus, most control schemes applied to improve characteristics of high-bandwidth active suspensions are nonlinear controllers.

On the other hand, it has been shown in [5] that the regulated quantity should be selected carefully in order to assure system stability and avoid oscillatory behavior of the high-bandwidth active suspension. The above discussion shows the complexity of control the high bandwidth active suspension and the need for advanced nonlinear techniques (aerospace technology and components), [6], [8], to control such system and thus the need of microprocessors to hold needed computations and adaptations. In this study we introduce linear control techniques to achieve good performance characteristics for the active suspension. Linear controllers such as PID are still the most preferable in industry in addition to its ease of tuning without getting involved in complex mathematical model of controlled system.

A brief review of some studies that applied low bandwidth active suspension and main results and improvements achieved will be shown following, then we show some high bandwidth suspension studies that employed the full nonlinear electro-hydraulic actuator dynamics.

2.2. REVIEW OF LOW BANDWIDTH ACTIVE SUSPENSIONS STUDIES

Some studies of low bandwidth active suspensions with emphasis on power needs considerations are shown here. Most of these studies apply adaptive techniques with linear adaptation functions to improve low frequency response of suspension. In general, the following studies didn't show response of vehicle handling for their approaches.

In 1992, Shuttlewood, Crolla, and Sharp, [8], showed that low bandwidth active suspensions still more suitable for mass product in automotive industry. Also, their power consumptions are lower than that of high bandwidth suspensions as their operating frequency is low (3 Hz) compared to (12 Hz) for high bandwidth ones.

1n 1994, Williams and Best, [6], and Williams, [4], tested a low bandwidth suspension with a dynamic leveling control that levels car body rapidly through a closed loop control with a modified skyhook damping. The system gave an improvement in transmitted accelerations to car body by a reduction of 8% for high frequency disturbances and 58% for low frequency disturbances compared to passive suspensions. The study showed that their system power needs ranges from 500 watts to 7.5 kilowatts according to driving conditions.

In 1994, Truscott and Burton, [9] also tested a low bandwidth suspension using a similar dynamic leveling philosophy by applying a multi-loop PID control. Nonlinearities of their system components were modeled. Also, their study focused on modeling of the suitable test road profile to examine suspension response in addition to modeling inertial disturbances affecting suspension during cornering.

In 1995, Appleyard and Wellstead, [1], gave a good background to active suspensions and noticed a brief historical information about vehicle suspensions in general and cited technologies used by vehicles' manufacturers and trends in the field of active suspensions concerning components and control strategies.

More studies and approaches applied to low bandwidth active suspensions can be found in [3], [10], [11], and [12].

2.3. REVIEW OF HIGH BANDWIDTH ACTIVE SUSPENSIONS STUDIES

Review of high bandwidth active suspensions is shown here to demonstrate a background regarding actuator dynamics used in active suspensions. Many studies employed full nonlinear dynamics of the electro-hydraulic actuator and most of these studies used the same analysis in modeling actuator dynamics following Merritt, [13]. Also, a similar road disturbance function was applied in most of these studies, which will give us a comparison reference.

1n 1992, [14] and 1995, [15], Alleyne and Hedrick employed full nonlinear actuator dynamics with adaptive control schemes based on Lyapunov analysis. The

adaptive sliding control used in their study was set to track needed actuator forces. Their studies showed notable improvements in ride quality of the suspension performance.

In 1997, Lin and Kanellakopoulos, [5], introduced a backstepping control to form a nonlinear filter to switch between soft setting of actuator force in small suspension deflections and a hard setting when suspension limits are reached in order to avoid hitting suspension limits. Full nonlinear dynamics of the hydraulic actuator were employed in their study. A reference road disturbance signal was introduced in this study that has been used later in many following studies as a reference base for comparison of performance characteristics. The study showed superior improvements by reduction of car body acceleration by 70% and reduction of car body travel by 80% compared to passive suspension.

In 2002, Fialho and Balas, [7], introduced an adaptive approach based on (Linear Parameter Varying) for a gain-scheduling control and combination with backstepping control. The adaptation was made to the nonlinear characteristics of the suspension based on road condition. Also, full nonlinear dynamics of the actuator were employed. Car body acceleration achieved was reduced by about 50% compared to passive suspension.

In 2004, Lin and Huang, [16], introduced a half car model with applying the same nonlinear backstepping technique introduced in [5] and test half-car response for the applied technique.

In 2006, Sam and Osman, [19], introduced a Proportional-Integral Sliding Mode Control (PI/SMC) to improve ride handling through control of actuator force. Robustness of the system was improved to handle uncertainties.

Also in 2006, Sam and Hudha, [20], divided control scheme into two control loops; the outer loop one was to calculate the needed actuator force through a PI/SMC controller introduced in [19], and the inner loop forms a PI control to drive the actuator force close to that generated by the PI/SMC control. This improved system robustness but slightly increased wheel travel.

In 2008, Sam, Suaib, and Osman, [23], tested the PI/SMC control for a half-car model for different road conditions and showed that it was completely insensitive to road disturbances irregularities. Also, robustness of the control system was improved. Simulations showed a reduction in car body acceleration by about 75% compared to passive one.

In 2010, Hassanzadeh, Alizadeh, Shirjoposht, and Hashemzadeh, [25], developed a nonlinear optimal controller based on a quadratic cost function. A full nonlinear dynamic model of the hydraulic actuator was used in the study for a half-car suspension model. Results obtained showed notable improvements in ride quality by reduction of car body acceleration by about 75% compared with passive suspension.

In 2011, Ekoru, Dahunsi, and Pedro, [26], introduced a PID control scheme for force tracking control after dividing the system into two loops; outer loop for determining needed actuator force, and inner loop for force tracking. The technique was applied to a half-car model with employing full actuator dynamics. The main index achieved by this study was settling the car body as fast as possible, i.e.,

minimization of settling time and this gave the ability to cut the vibration exposure time by half and return the body to its original state. This maintained accepted passenger comfort level.

2.4. SUMMARY OF LITERATURE REVIEW

Previous studies showed that low bandwidth active suspensions are more applicable for mass product in automotive industry. Also, their energy consumptions are lower than that of high bandwidth ones. Known low bandwidth studies lasted only for about ten year, from 1986 to 1996, and no further studies held later which may be confusing since studies in this field have demonstrated a good base to justify using low bandwidth suspensions in industry.

On the other hand, most of the above mentioned studies in low bandwidth suspensions didn't apply a reference road condition to demonstrate a general base of comparison, but they applied random signals with different frequencies to test their systems.

High bandwidth suspensions need complex mathematics and control design and need an aerospace technology and components to be attached to vehicles which may not be justified from an industrial point of view in addition to their high energy consumption and low economic feasibility. However, cited studies employed the full nonlinear dynamics to model the hydraulic actuator with the same parameters which will give a general comparison base. Also, test inputs for these studies were similar.

In order to achieve good performance characteristics of the active suspension, we have proposed a special structure of the low bandwidth active suspension. Nonlinear actuator dynamics will be employed in the proposed low bandwidth suspension. A new PID with fuzzy switch control scheme will be used in order to improve performance over conventional passive suspension. Also, conventional and optimized PID control schemes will be introduced.

3. SYSTEM DESIGN AND CONTROL

3.1. INTRODUCTON

In this chapter we introduce our proposed suspension first for a quarter car model and the design of control strategies for such system, then we expand our analysis and design for a half-car model.

3.2. PROPOSED SUSPENSION SYSTEM FOR QUARTER CAR

Our proposed system is a special structure of the low bandwidth active suspension system. We propose that a hydraulic actuator to be placed above the sprung mass, which will be assumed a disc with a small mass value relative to car chassis mass.

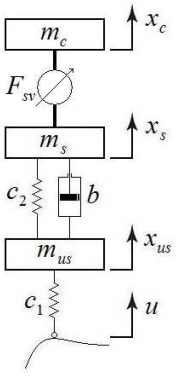

Figure (3.1): Proposed quarter car active suspension system.

As shown in Fig. 3.1, car body, m_c, is to be supported only by the hydraulic actuator while the passive suspension components will remain the same. The sprung

mass, m_s, represents a small disc-like mass with appropriate mechanical hardness to support the hydraulic actuator. This mass will be helpful in slowing road disturbances transfer to car chassis and this would give our controller the time to be able to track road profile. Unsprung mass, m_{us} represents wheel assembly. The spring, c_2, the damper, b, and spring, c_1, represent stiffness of passive spring, stiffness of passive damper, and stiffness of pneumatic compressed tire, respectively. The variables u, x_{us}, x_s, x_c represent road disturbance profile, wheel travel, disc travel, and body travel, respectively. The force F_{sv} generated between sprung mass and car body is built up by pressure difference across a hydraulic actuator. Hydraulic actuator is taken here to be a four-way critically lapped spool valve controlled by a flapper valve with force feedback, the same as in [5], [7], and [14]. The force generated by the actuator can be written as

$$F_{sv} = A.P_L \qquad (3.1)$$

where A is the cross sectional area of the actuator cylinder piston and P_L is pressure drop across cylinder piston. As shown in [13] the change in pressure drop can be written as

$$\frac{V_t}{4\beta_e}\dot{P}_L = Q_L - C_{tp}P_L - A(\dot{x}_c - \dot{x}_s), \qquad (3.2)$$

where V_t is total actuator volume, β_e is the effective bulk modulus, Q_L is hydraulic fluid flow, and C_{tp} is the total leakage coefficient of the piston. The fluid flow is given by

$$Q_L = \mathrm{sgn}[P_s - \mathrm{sgn}(x_v)P_L]C_d w x_v \sqrt{\frac{1}{\rho}|P_s - \mathrm{sgn}(x_v)P_L|} \qquad (3.3)$$

where C_d is discharge coefficient, w is spool valve area gradient, x_v is displacement of spool valve, ρ is hydraulic fluid density, and P_s is hydraulic supply pressure. The spool valve displacement is controlled by a voltage or current input r to the servo valve. The dynamics of the servo valve can be approximated by a linear filter as

$$\dot{x}_v = \frac{1}{\tau}(-x_v + r) \qquad (3.4)$$

Now, the mathematical model of the proposed quarter car suspension using Newton's second law, along with the full dynamics of the hydraulic actuator shown in equations (3.1) to (3.4) will be:

$$
\begin{aligned}
\ddot{x}_{us} &= \frac{1}{m_{us}}[c_2(x_s - x_{us}) + b(\dot{x}_s - \dot{x}_{us}) - c_1(x_{us} - u)] \\
\ddot{x}_s &= \frac{1}{m_s}[-c_2(x_s - x_{us}) - b(\dot{x}_s - \dot{x}_{us}) + AP_L] \\
\ddot{x}_c &= \frac{1}{m_c}[-AP_L] \\
\dot{P}_L &= -\beta P_L - \alpha A(\dot{x}_c - \dot{x}_s) + \gamma x_v w_s
\end{aligned}
\tag{3.5}
$$

where

$$
\begin{aligned}
&\alpha = \frac{4\beta_e}{V_t}, \quad \beta = \alpha C_{tp}, \quad \gamma = \alpha C_d w \sqrt{\frac{1}{\rho}}, \quad \textit{and} \\
&w_s = \operatorname{sgn}[P_s - \operatorname{sgn}(x_v)P_L]\sqrt{|P_s - \operatorname{sgn}(x_v)P_L|}
\end{aligned}
\tag{3.6}
$$

Proposed active suspension shown in Fig. 3.1 with governing equations (3.5) and (3.6) is built as shown in Fig. 3.2 below

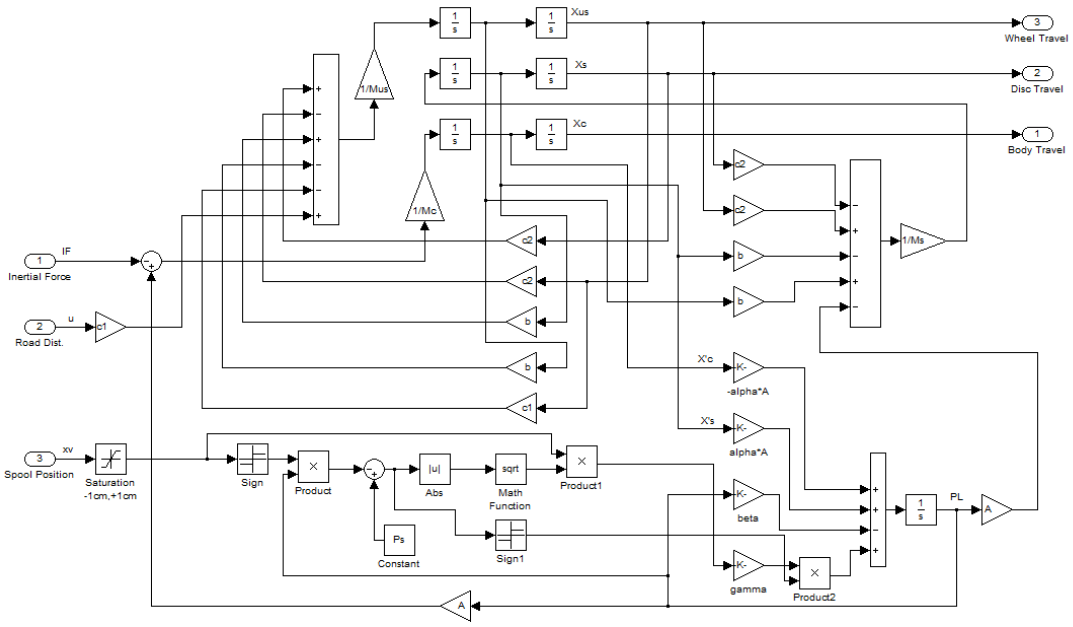

Figure (3.2): Proposed active suspension SIMULINK model.

Note the inertial force modeled within the diagram as a negative force value added to the acceleration equation of the car body. This input will form the inertial disturbance that will applied to the suspension throughout the study. Inputs to our model are: inertial force, road disturbance, and spool displacement which is set by our control signal according to the electro-hydraulic servo valve dynamics shown in equation (3.4).

Electro-hydraulic servo valve dynamics are modeled as shown in Fig 3.3

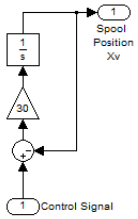

Figure (3.3): Electro-hydraulic servo valve dynamics.

3.3. CONTROL STRATEGIES AND DESIGN

The control problem we need to solve here can be considered a disturbance rejection problem where road and load variations should not disturb passenger comfort neither vehicle stability. In this section we show design procedure and justify our proposed structure and show that linear control schemes will be enough to handle regulation of this system. Our analysis and control design is applied to quarter-car model, then the control scheme is applied in the same manner to every wheel individually. The proposed structure for each quarter car suspension forms two series components; passive suspension and hydraulic actuator. The main idea of this proposed suspension is to drive the hydraulic actuator as a displacement compensator for variation of road level or in case of body roll or pitch movements.

3.3.1. Stability of proposed quarter-car active system:

In order not to get undesirable behavior of the closed-loop system, we need to perform analysis for our proposed system to check that it is stable. Our stability analysis is performed as illustrated in [5] and is shown below.

If we assume our goal is to minimize forces transferred to passenger, i.e. minimization of car body accelerations then, we need to realize $\ddot{x}_c = 0$ and to have no forces applying on car body which will yield to

$$P_L = 0 \qquad (3.7)$$

Substituting of this value in system shown in equation (3.5) results in

$$\begin{aligned} \ddot{x}_{us} &= \frac{1}{m_{us}}[c_2(x_s - x_{us}) + b(\dot{x}_s - \dot{x}_{us}) - c_1(x_{us} - u)] \\ \ddot{x}_s &= \frac{1}{m_s}[-c_2(x_s - x_{us}) - b(\dot{x}_s - \dot{x}_{us})] \qquad (3.8) \\ \ddot{x}_c &= 0 \end{aligned}$$

Note that equation (3.8) represents a passive suspension system which is stable. That is, as control signal goes to zero the remaining system will behave as a passive suspension which is stable. Also, if we want to consider minimization of car body displacement the analysis will be similar to that in equations (3.7) and (3.8).

In the rest of this chapter we apply two different control strategies; in the first one we use PID control to compensate any variation of passive suspension deflection with a fuzzy controller to perform switching between positive and negative compensation as will be discussed in the following section, while in the second one we regulate car body travel only through PID control schemes.

3.3.2. PID control with fuzzy switch scheme:

The proposed suspension structure gives us the advantage of that, at any fault in active suspension, conventional suspension will remain operating. In this section we show design procedure and justify our proposed structure and control. Our analysis and control design is applied to quarter-car model, then the control scheme can be applied in the same manner to every wheel. As mentioned previously in this chapter, our main idea of suspension is to compensate variations in passive suspension deflection.

In order to realize this compensation, we will use the deflection of the passive suspension part (x_s-x_{us}) as the reference value of the hydraulic cylinder length. This choice of input needs different reactions of our control scheme depending on whether the disturbance is road induced or inertial load induced. That is, if suspension deflection is negative due to a positive road disturbance then the hydraulic cylinder rod would contract in order to prevent transferring wheel travel to car body as possible. But this compensation should be inversed if the disturbance was due to inertial disturbance. That is, an inertial disturbance acting on car body downwards will cause the suspension deflection to have a negative value, but the cylinder rod here should extend not like the previous case, as the previous reaction for this case would double the effect of inertial disturbance. The problem here is to give the suspension system some intelligence in order to determine if the disturbance applied is road induced or inertial load induced since each case needs a different control reaction.

Our system can be implemented by attaching accelerometers to car body, sprung mass, and unsprung mass as shown in Fig. 3.4 to get all needed measurements of vertical velocity or displacement for any mass of the system. Following we introduce designs for bump rejection and load rejection control loops and then we will set the switching criteria between the two control strategies. In all cases we suppose that *reference value of car body displacement is zero*.

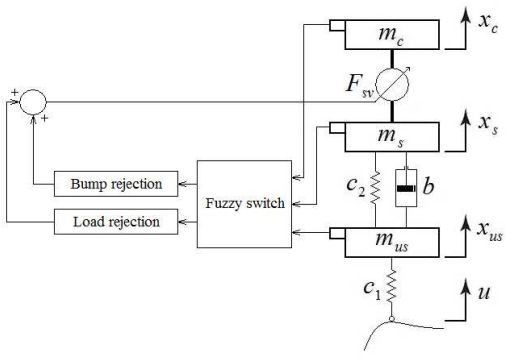

Figure (3.4):PID with fuzzy switch control scheme.

3.3.2.1. Bump rejection strategy:

This control scheme uses the passive suspension deflection (x_s-x_{us}) as input through a proportional control. Also, a PID control for the error of car body displacement (-x_c) is applied to assure that final car body displacement is zero. The control law for bump rejection can be written as

$$r_1 = K_{sv}\{k_d(x_s(t) - x_{us}(t)) + 0.5[-K_P x_c(t) - K_I \int x_c(t)dt - K_D \frac{dx_c(t)}{dt}]\} \qquad (3.9)$$

where K_P, K_I, K_D are PID controller gains and k_d and K_{sv} are scaling gains corresponding to deflection and servo valve, respectively, and all these gains are tuned by trial and error.

Note that this control law will behave undesirably for inertial disturbances as discussed earlier. Thus, bump rejection strategy can be effective only to isolate road disturbances.

3.3.2.2. Load rejection strategy:

This control uses the error of car body displacement (-x_c) as input for the controller and the control law is the same PID controller used for bump rejection strategy

$$r_2 = K_{sv}[-K_P x_c(t) - K_I \int x_c(t)dt - K_D \frac{dx_c(t)}{dt}] \qquad (3.10)$$

3.3.2.3. Switching algorithm, fuzzy switch:

This algorithm forms the knowledge base of the suspension system and would give the suspension the intelligence to decide whether to operate bump rejection or load rejection strategy. This is achieved by a novel fuzzy controller with five inputs and two outputs. Inputs are car body displacement and velocity, (namely Xc and dXc), sprung mass displacement and velocity, (namely Xs and dXs), in addition to passive suspension deflection, (Xs-Xus). The outputs are 'Bump' and 'Load'.

All inputs are given linguistic variables as: 'N', for negative value and 'P', for positive value. Outputs are given linguistic variables as: 'Zero', for "0" output and 'One', for "1" output. As shown in Fig. 3.5, input displacements are given a range in the interval [-0.25, 0.25] with trapezoidal membership functions (MF's) while velocities range is [-1, 1] with trapezoidal MF's and outputs are selected to have either 'Zero' or 'One' with triangular MF's.

Membership functions for displacements are: trap(-0.3,-0.3,0,0) for 'N' and, trap(0,0,0.3,0.3) for 'P'. While MF's for velocities are: trap(-1.1,-1.1,0,0) for 'N' and, trap(0,0,1.1,1.1) for 'P'. Output MF's are: tri(0,0,0) for 'Zero' and tri(1,1,1) for 'One'.

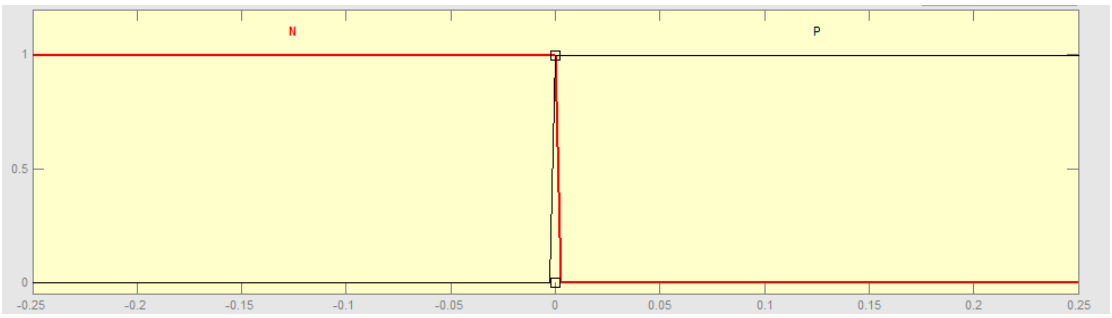

a)

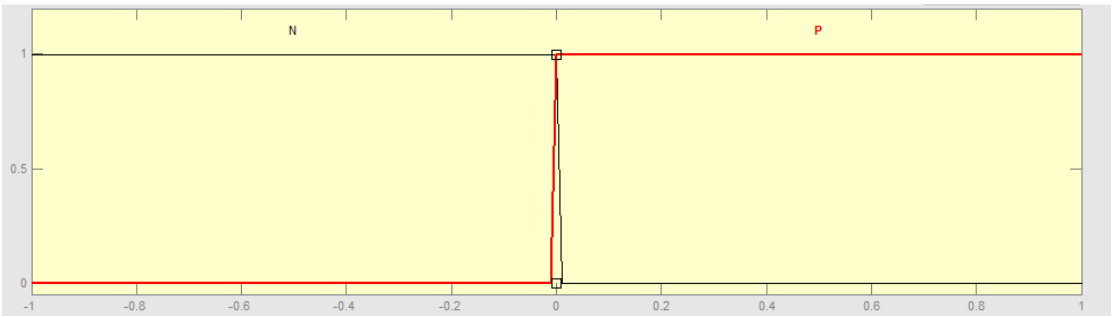

b)

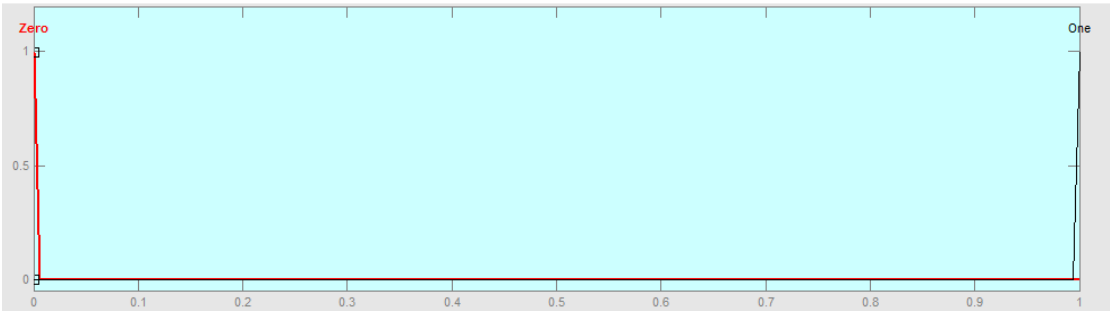

c)

Figure (3.5): Membership functions for: a) displacements (Xc, Xs, and Xs-Xus), b) velocities (dXc, dXs), c) outputs (Bump, Load).

Defuzzification is performed using *Mamdani* method with applying centroid defuzzification method in order to generate fuzzy control value. The fuzzy control law is in the form:

IF "In1" is "Ix" AND "In2" is "Iy" AND …..THEN "O1" is "Ox" and "O2" is "Oy".

where IN1 refers to input 1, IX is corresponding value to this input, O1 refers to output 1, OX is corresponding value to this output, etc. Designed rule base is shown in Table 3.1 below.

For example, rule number 1 can be said to be

IF "Xc" is "N" AND "dXc" is "N" AND "Xs" is "N" AND "dXs" is "N" AND "Xs-Xus" is "N", THEN "Bump" is "Zero" and "Load" is "One".

Table (3.1): Rule base of fuzzy controller.

	Xc	dXc	Xs	dXs	Xs-Xus	Bump	Load
1	N	N	N	N	N	Zero	One
2	P					One	Zero
3	N	P				Zero	Zero
4	P					One	Zero
5	N	N	P			Zero	One
6	P					One	Zero
7	N	P				One	Zero
8	P					One	Zero
9	N	N	N	P		Zero	One
10	P					One	Zero
11	N	P				Zero	One
12	P					One	Zero
13	N	N	P			Zero	One
14	P					One	Zero
15	N	P				One	Zero
16	P					One	Zero

Note that only shaded rules shown in rule base are the cases where bump rejection is deactivated and note rule number 3 where this situation is treated passively. Also, for all positive values of suspension deflection the output will be in bump rejection mode.

Outputs of fuzzy controller may have values of "0" or "1". Assuming "Bump" output value to be "B" and "Load" output value to be "L", then the final control law is

$$r = Br_1 + Lr_2 \qquad (3.11)$$

PID with fuzzy switch control strategy discussed in this section is implemented by applying control law described in equation (3.11) as shown in Fig. 3.6 below. Control scheme is built as shown in Fig. 3.7 according to that shown in Fig. 3.4. Controller output is filtered to reject high frequency control signals that may occur from high frequency switching. Low pass filter is used with pass edge at 200 rad/sec to prevent undesirable switching.

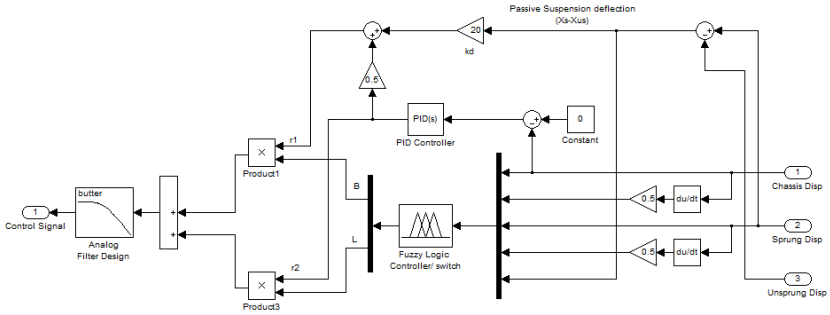

Figure (3.6): Controller/ selector generating control law.

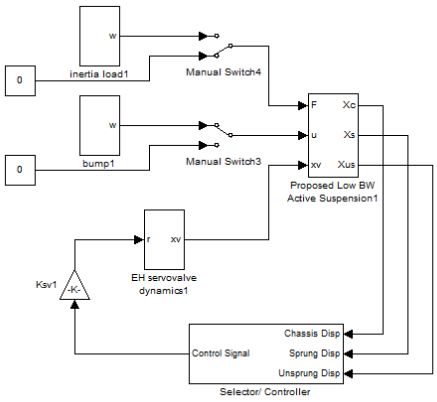

Figure (3.7): PID with fuzzy switch control scheme.

3.3.3. PID control:

This control scheme is applied to regulate car body displacement by closing our control loop with the value of car body travel only. Our reference input for car body travel is *zero* and road variations or load variations are considered as disturbances in the control loop. Schematic diagram of this control is shown in Fig. 3.8 below

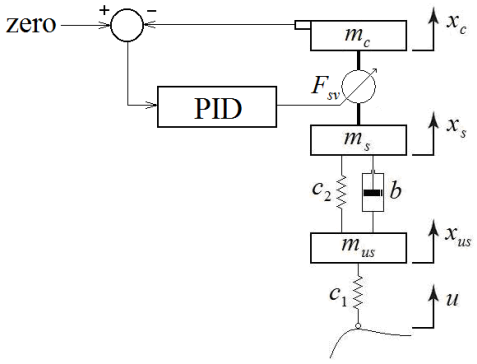

Figure (3.8): PID control scheme for car body.

Our control law for this case is

$$r = K_{sv}[-K_p x_c(t) - K_i \int x_c(t)dt - K_d \frac{dx_c(t)}{dt}] \qquad (3.12)$$

Assuming that our reference value for car body displacement is *zero*. Note that PID gains here are different from those shown in control laws of equations (3.9) and (3.10). Setting of control law values shown in equation (3.12) is performed by two ways throughout this study; first by tuning conventional PID control parameters by trial and error, and the second is by the use of *SIMULINK Design Optimization* tool.

This tuning is performed using the *SIMULINK Design Optimization* tool supported by MATLAB®. Procedure of tuning PID parameters tuning is done by setting our desired car body level to some value, say 0.01 m, and performing iterative optimization problem for achieving desired step response characteristics, as shown in Fig. 3.9. This is done using *Signal Constraint* block with specifying our tuned parameters to be the PID controller gains K_p, K_i, and K_d. Note that we have chosen to have a rapid response with very small rise and settling times in order to cut vibration disturbances as fast as possible. But this forced us to widen the accepted overshoot range up to 40%.

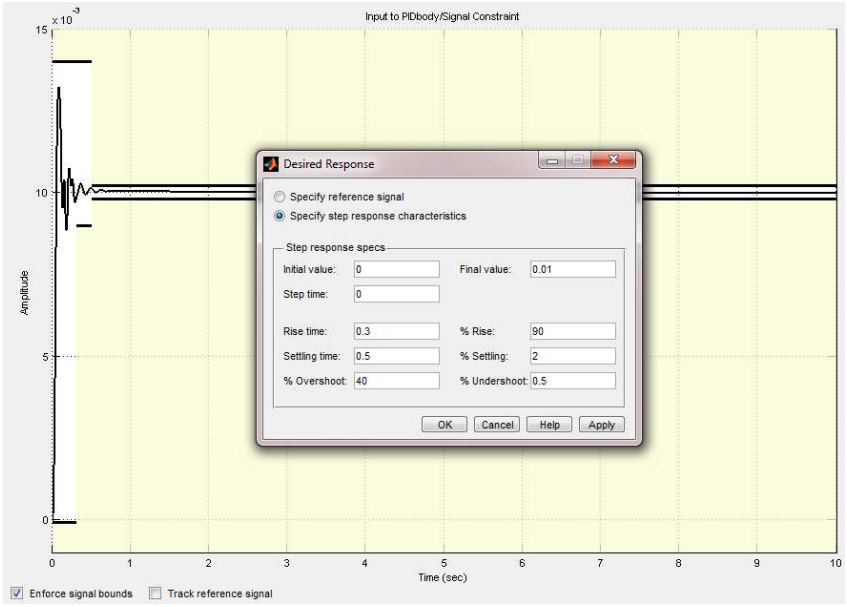

Figure (3.9): Desired step response for optimized PID control.

Desired response is set to have the following bounds shown in Table (3.2)

Table (3.2): Desired step response characteristics for optimized PID control.

Characteristics			
Rise time (sec)	0.3	% Rise	90
Settling time (sec)	0.5	% Settling	2
% Overshoot	40	% Undershoot	0.5

PID control scheme described in equation (3.12) and shown in Fig. 3.8 is implemented as shown in Fig. 3.10 below

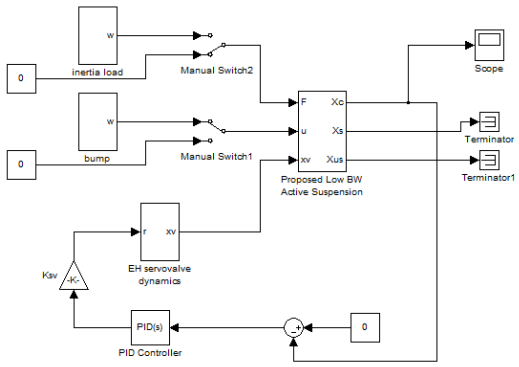

Figure (3.10): PID control scheme.

3.4. HALF-CAR MODEL AND CONTROL

Now we extend model analysis for a half-car case shown in Fig. 3.11 where car chassis, m_c, is to be supported only by the hydraulic actuators while the passive suspension components will remain the same. In Fig. 3.11 the sprung masses, m_f and m_r, represent the small disc-like masses. Unsprung masses, m_{uf} and m_{ur} represent front and rear wheel assemblies, respectively. The springs, c_f and c_r, the dampers, b_f and b_r, and springs, c_{tf} and c_{tr}, represent stiffness of passive springs, stiffness of passive dampers, and stiffness of pneumatic compressed tires, for front and rear assemblies, respectively. The variables u_f, x_{uf}, x_{sf}, x_f represent road disturbance, wheel travel, disc travel, and body travel of the front side, respectively and variables u_r, x_{ur}, x_{sr}, x_r represent road disturbance, wheel travel, disc travel, and body travel of the rear side, respectively.

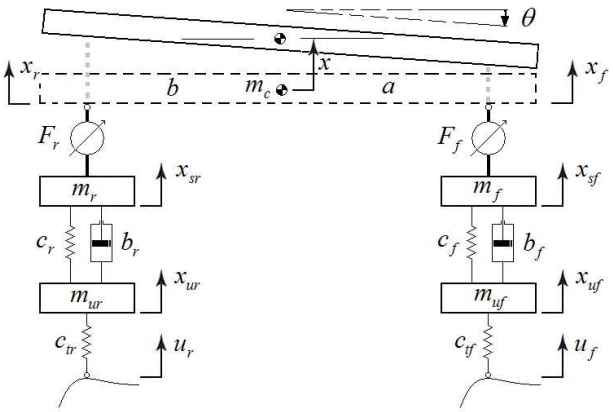

Figure (3.11): Proposed half-car active suspension system.

The forces F_f and F_r generated between sprung masses and car body are built up by pressure difference across a hydraulic actuators and the forces generated by actuators can have the general form, similar to equation (3.1)

$$F_i = A.P_{Li}, \quad i = f, r \qquad (3.13)$$

and the change in pressure drops can be written as

$$\frac{V_t}{4\beta_e}\dot{P}_{Li} = Q_{Li} - C_{tp}P_{Li} - A(\dot{x}_i - \dot{x}_{si}), \quad i = f, r \qquad (3.14)$$

where the fluid flows are given by

$$Q_{Li} = \text{sgn}[P_s - \text{sgn}(x_{vi})P_{Li}]C_d w x_{vi}\sqrt{\frac{1}{\rho}|P_s - \text{sgn}(x_{vi})P_{Li}|}, \quad i = f, r \qquad (3.15)$$

and the pressure drops across actuators can be described by

$$\dot{P}_{Li} = -\beta P_{Li} - \alpha A(\dot{x}_i - \dot{x}_{si}) + \gamma x_{vi} w_s, \quad i = f, r \qquad (3.16)$$

where,

$$\alpha = \frac{4\beta_e}{V_t}, \beta = \alpha C_{tp}, \gamma = \alpha C_d w\sqrt{\frac{1}{\rho}}, \quad and$$
$$w_s = \text{sgn}[P_s - \text{sgn}(x_{vi})P_{Li}]\sqrt{|P_s - \text{sgn}(x_{vi})P_{Li}|} \qquad (3.17)$$

The spool valve displacements are controlled by voltage or current inputs r_i to the servo valves. The dynamics of the servo valves can be approximated by a linear filter as

$$\dot{x}_{vi} = \frac{1}{\tau}(-x_{vi} + r_i), \quad i = f, r \qquad (3.18)$$

Now, following [16] the mathematical model of the proposed half-car suspension using Newton's second law, along with the full dynamics of the hydraulic actuator shown in equations (3.13) to (3.18) will be:

for unsprung masses (wheels)

$$\ddot{x}_{ui} = \frac{1}{m_{ui}}[c_i(x_{si} - x_{ui}) + b_i(\dot{x}_{si} - \dot{x}_{ui}) - c_{ti}(x_{ui} - u_i)], \quad i = f, r \qquad (3.19)$$

for sprung masses (discs)

$$\ddot{x}_{si} = \frac{1}{m_i}[-c_i(x_{si} - x_{ui}) - b_i(\dot{x}_{si} - \dot{x}_{ui}) + AP_{Li}] \qquad (3.20)$$

while the dynamics of motion for the front side of car body can be described by

$$\ddot{x}_f = \frac{1}{m_c}[F_f + F_r - am_c\ddot{\theta}] \qquad (3.21)$$

and the dynamics of motion for the rear side of car body is

$$\ddot{x}_r = \frac{1}{m_c}[F_f + F_r + bm_c\ddot{\theta}] \qquad (3.22)$$

where F_f and F_r are shown in equations (3.13) and (3.16), a is the distance from the front axle to center of gravity of car body, b is the distance from the rear axle to center of gravity of car body, and θ is body pitch angle and can be described

$$\ddot{\theta} = \frac{1}{J_y}[-aF_f + bF_r] \qquad (3.23)$$

where J_y is moment of inertia of car body. Note that positive direction of pitch angle is assumed to be clock wise. Finally, travel of center of gravity of car body can be calculated by

$$x = x_f + a\sin\theta = x_r - b\sin\theta \qquad (3.24)$$

Now the full dynamics of the half-car model is described. Control of half-car model is achieved by applying control strategies shown earlier in this chapter for each quarter-car individually.

For modeling half-car in SIMULINK environment, the same quarter car model shown in Fig. 3.2 is copied for the second wheel. Half car model differs from quarter car in treating with the car body mass which will be supported here by two forces and with taking into consideration the mutual reactions between the front and rear sides when moving. Thus, in Fig. 3.12 we show only the main block diagram used to simulate equations (3.21) to (3.24)

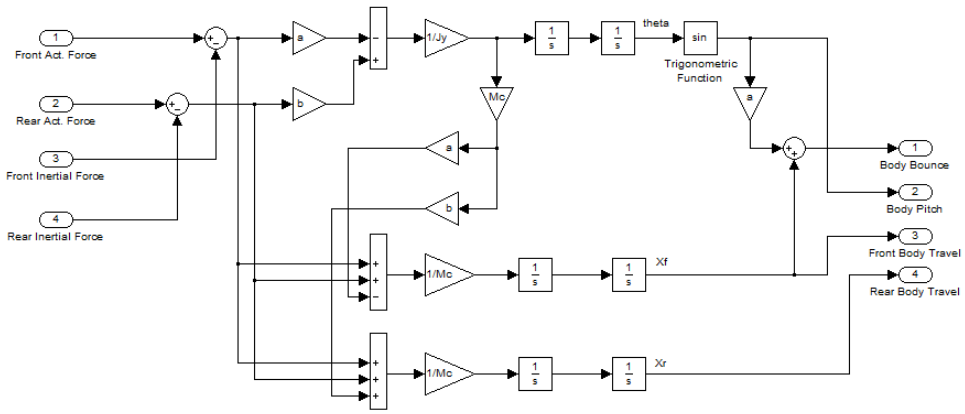

Figure (3.12): Simulating body bounce and pitch angle for a half car model.

3.5. POWER REQUIREMENTS AND ENERGY CONSUMPTIONS OF ACTIVE SUSPENSIONS

Back to the name of *active suspensions*, energy is injected to these systems to drive them towards achieving our desired performance characteristics (see *Section* 2.3). Thus, in this section we show calculations of power needs for our proposed active suspensions in order to compare power needs values for each of our proposed control strategies discussed in this chapter. Also, calculation of total energy consumed by the active actuator will be shown.

Active element in suspension is the hydraulic cylinder and the mechanical power injected to the system is in the form of linear translational mechanical motion. For such motion, mechanical power can be calculated as

$$P(t) = F(t)v(t) \qquad (3.25)$$

where

$F(t)$ is the instantaneous force applied by the actuator and, $v(t)$ is the velocity of the piston relative to cylinder body. For the quarter-car model, assuming that the efficiency of the hydraulic system is ideal, instantaneous power requirements can be calculated by

$$P(t) = F_{sv}(t)[\dot{x}_c(t) - \dot{x}_s(t)] \qquad (3.26)$$

And for the half-car model, power requirement is

$$P(t) = F_f(t)[\dot{x}_f(t) - \dot{x}_{sf}(t)] + F_r(t)[\dot{x}_r(t) - \dot{x}_{sr}(t)] \qquad (3.27)$$

For some period of time t=[0, T], energy consumed by the actuator can be calculated by

$$E = \int_0^T P(t).dt \qquad (3.28)$$

To apply equations (3.26) and (3.28) in SIMULINK environment, block diagram shown in Fig. 3.13 is built

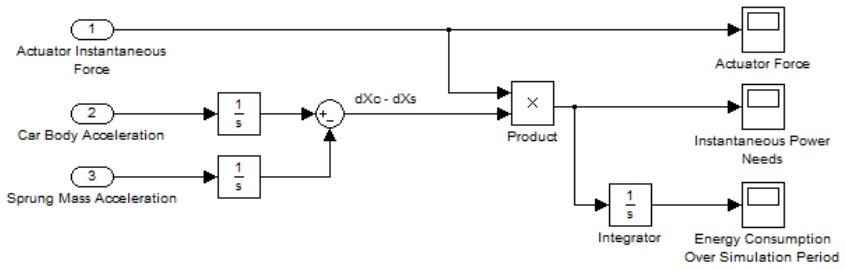

Figure (3.13): Block diagram for monitoring power needs and energy consumptions of active suspension.

In the following chapter, our different control strategies will be applied for similar driving conditions and comparison between suspension performance and power requirements and energy consumptions for each control strategy will be shown.

3.6. SYSTEM VISUALIZATION

Visualization is performed to give us better understanding when project budget is limited. Our visualization is set up through simple tools of MATLAB programming language in 2-D animation. Animation is performed by playing a sequence of figures with step movements to form a whole video capture. Sequence of figures is updated through a *for-loop*.

Data of our system response are saved into MATLAB workspace after running our SIMULINK model. Data of our concern are captured from SIMULINK using the block *To Workspace* with saving data in the form: *Structure with time*.

These data are called in our script and form data vectors with the same length, then viewed in steps to form the whole motion of the bodies in concern. Animation shows response of our active suspension compared to passive one as shown in Fig. 3.14. M-file script is shown in Appendix.

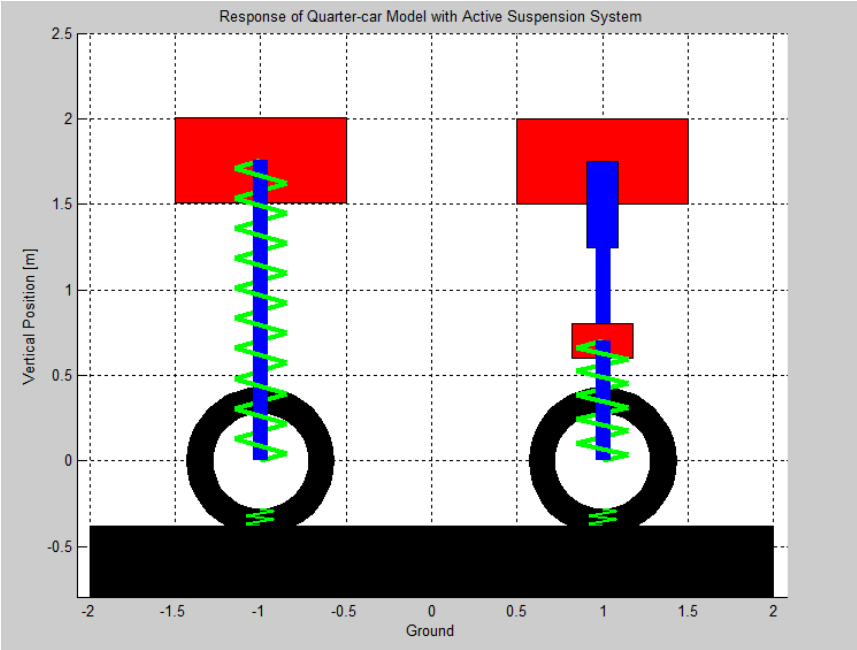

Figure (3.14): Suspension visualization.

4. SIMULATION RESULTS AND DISCUSSION

4.1. INTRODUCTION

In this chapter we show simulation results for our proposed suspension structure controlled by our control schemes discussed in *Chapter* 3. Control schemes are applied first to a quarter car model, then we extend simulation for a half-car model. All simulation results are compared with passive suspension response and improvements over previous studies are shown. Also, peak power requirements and energy consumption for each control scheme are shown.

4.2. SIMULATION RESULTS FOR A QUARTER CAR MODEL

Our proposed suspension with control strategy discussed is compared with passive suspension response for the same input. Using standard parameters and values taken from [14] and used in [5] and [7]:

$$\begin{aligned} &m_c = 290\,kg, \quad m_s = 20\,kg, \quad m_{us} = 59\,kg, \quad c_1 = 190000\,N/m, \quad c_2 = 16812\,N/m, \\ &b = 1000\,N/m/s, \quad \tau = 1/30\,\text{sec}, \quad P_s = 10342500\,Pa, \quad A = 3.35\times10^{-4}\,m^2, \\ &\alpha = 4.515\times10^{13}\,N/m^5, \quad \beta = 1\text{sec}^{-1}, \quad \gamma = 1.545\times10^{9}\,N/m^{5/2}kg^{1/2}. \end{aligned} \tag{4.1}$$

Note that value of sprung mass is set by trial and error and cannot be eliminated as it is important for our proposed suspension stability. Also, it is not justified to increase it bigger than this value due to extra weight of the car. Optimal selection of sprung mass value may be a separate research topic.

First we test system performance for a single road bump represented as

$$u(t) = \begin{cases} h(1-\cos 8\pi t), & 0.5 \le t \le 0.75 \\ 0, & otherwise \end{cases} \qquad (4.2)$$

Bump heights are said to be 5 cm and 11 cm, i.e. *h=0.025 and 0.055*. a sample of bump profile is shown in Fig. 4.1. Since Many previous studies showed that most important performance indexes for a good suspension system are; minimization of body vertical travel and acceleration which directly affect passenger comfort and, minimization of suspension deflection, i.e. relative displacement between sprung and unsprung masses which affects handling, [5], [7], [14]. Also, wheel hop is so important since it directly affects suspension handling in addition to force distribution of vehicle weight.

Thus, for each case we examine body travel, body acceleration, wheel travel, and suspension deflection (for our proposed active suspension, deflection is denoted by passive component deflection. This performance index is important because reaching suspension limits may damage vehicle components in addition to its discomfort effect to passengers. Note that throughout this study, displacement of servo valve spool is limited to ±1cm.

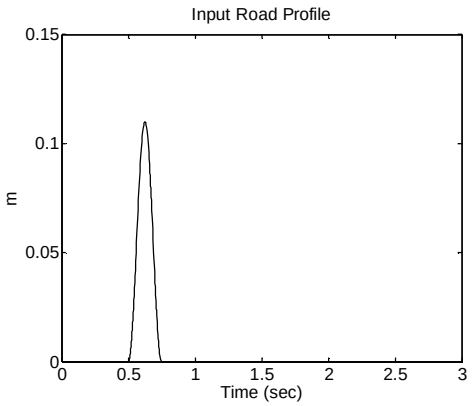

Figure (4.1): An 11 cm bump profile.

Road disturbance (bump) described in equation (4.2) is implemented as shown in Fig. 4.2 and is set to be a multiplication of two functions; first is a 4 Hz (ω=8π rad/sec), cosine wave shifted "+1" on the y-axis with a peak-to-peak value of "1" and the second forms a delayed unit step function to operate like an on/off switch. This function is set in many previous studies as this frequency exceeds the corner frequency of most of ground vehicle suspensions.

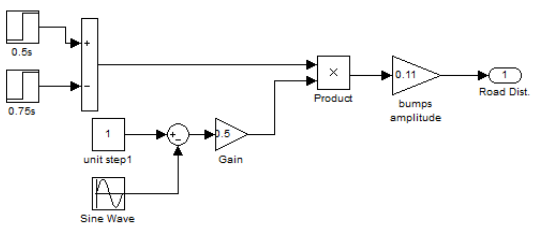

Figure (4.2): Road disturbance signal generator.

4.2.1. Response of PID with fuzzy switch control scheme:

Here we show response for the PID with fuzzy switch control scheme shown in *Section* 3.3.2 with input road profile represented in equation (4.2). With the use of the following control parameters to get our control laws shown in equations (3.9), (3.10), and (3.11)

$$K_{sv}=0.01,\ k_d=20,\ K_P=3.9,\ K_I=0.0001,\ \text{and}\ K_D=3 \qquad (4.3)$$

In Figure 4.3 response for a 5 cm bump is shown. Note that acceleration has been reduced by almost 60% and body travel by almost 93% compared to passive suspension. Also, handling performance still within accepted region, [2].

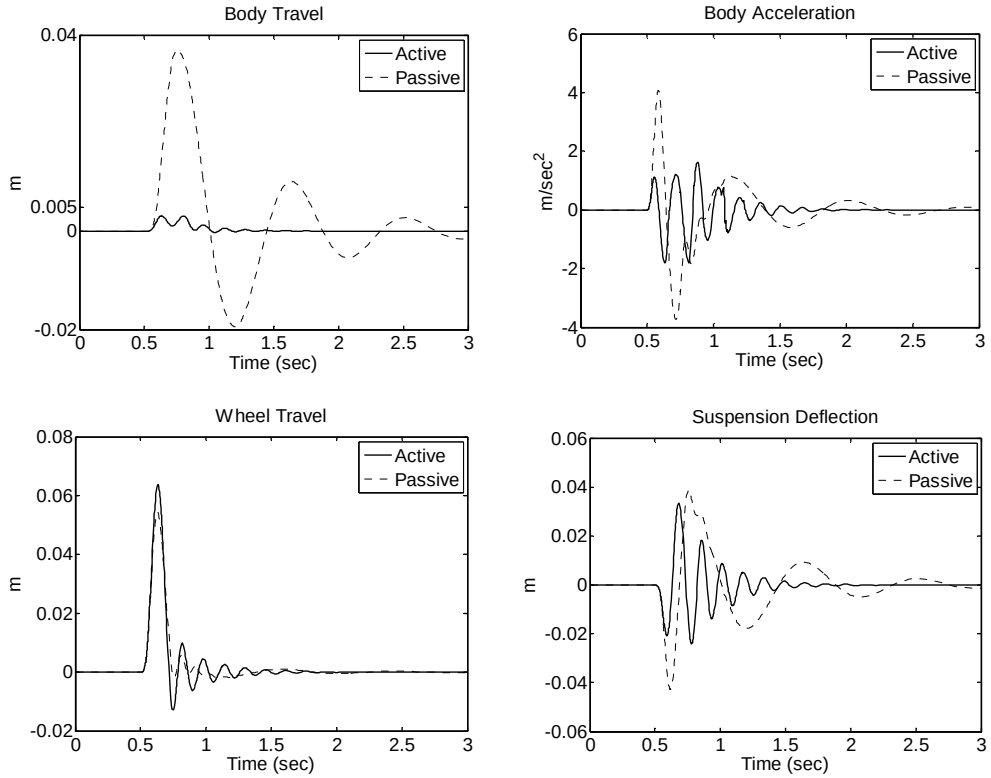

Figure (4.3): Quarter-car response of a PID with fuzzy switch control for a 5 cm bump.

When bump height is increased to 11 cm, response is better relatively for body acceleration as shown in Fig. 4.4. Note that acceleration is reduced by 70% and body travel by 91% of passive response. This gives more comfort for the passengers.

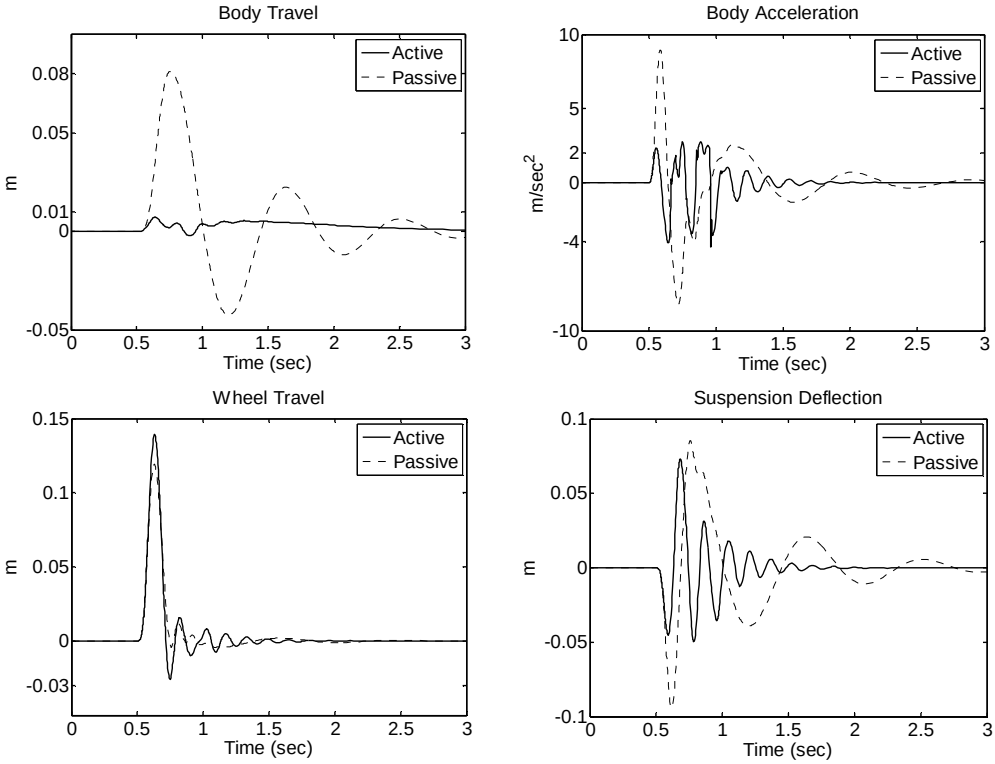

Figure (4.4): Quarter-car response of a PID with fuzzy switch control for an 11 cm bump.

Our proposed suspension performance is also tested for inertial disturbances by applying a force to the body mass acting downwards for some time period, [10]. The input force is applied to model dynamics and it is given a value according to the following function

$$IF(t) = \begin{cases} 300(1-\cos 2\pi t), & 1 \le t \le 1.5 \\ 600, & 1.5 \le t \le 5.5 \\ 300(1-\cos 2\pi t), & 5.5 \le t \le 6 \\ 0, & otherwise \end{cases} \qquad (4.4)$$

which can be represented as shown in Fig. 4.5 below.

Inertial force value was calculated in previous studies for a medium size cars when passing a curve with a 0.4g centrifugal acceleration which cause a force of about 600 N applying on the outer wheel passing the curve.

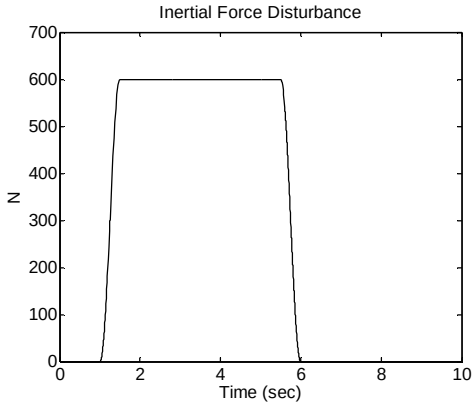

Figure (4.5): Inertial force disturbance.

Inertial force is modeled in SIMULINK as shown in Fig. 4.6 to have an s-shaped rising and falling edges which are half of a 1-Hz cosine wave described in equation (4.4)

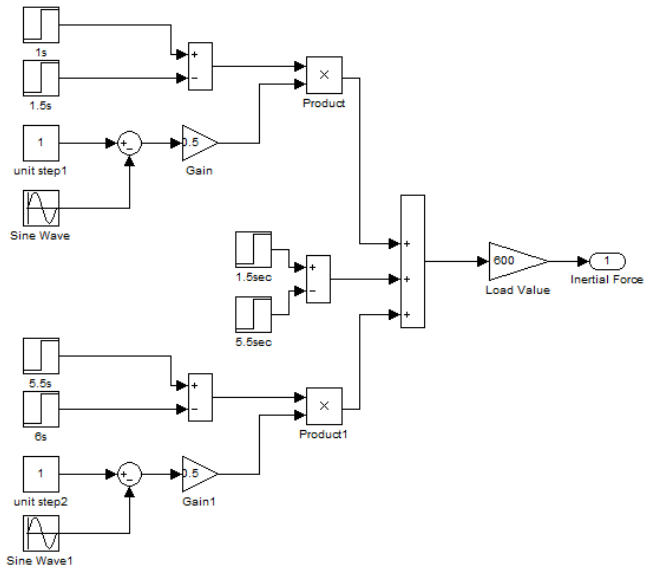

Figure (4.6): Inertial force signal generator.

Results shown in Fig. 4.7 show reaction for our proposed suspension structure and switching algorithm and this improved handling characteristics by preventing body roll or pitch movements, but response of this control/ switch is undesirable when load is released. This is due to the nature of our proposed fuzzy controller which acts as an on/off switch with applying a high gain proportional control when bump rejection strategy is activated. This may lead to unsatisfactory response for some cases. However, the acceleration positive values still acceptable, but the large negative acceleration values lead to a large wheel hops and these affect handling characteristics.

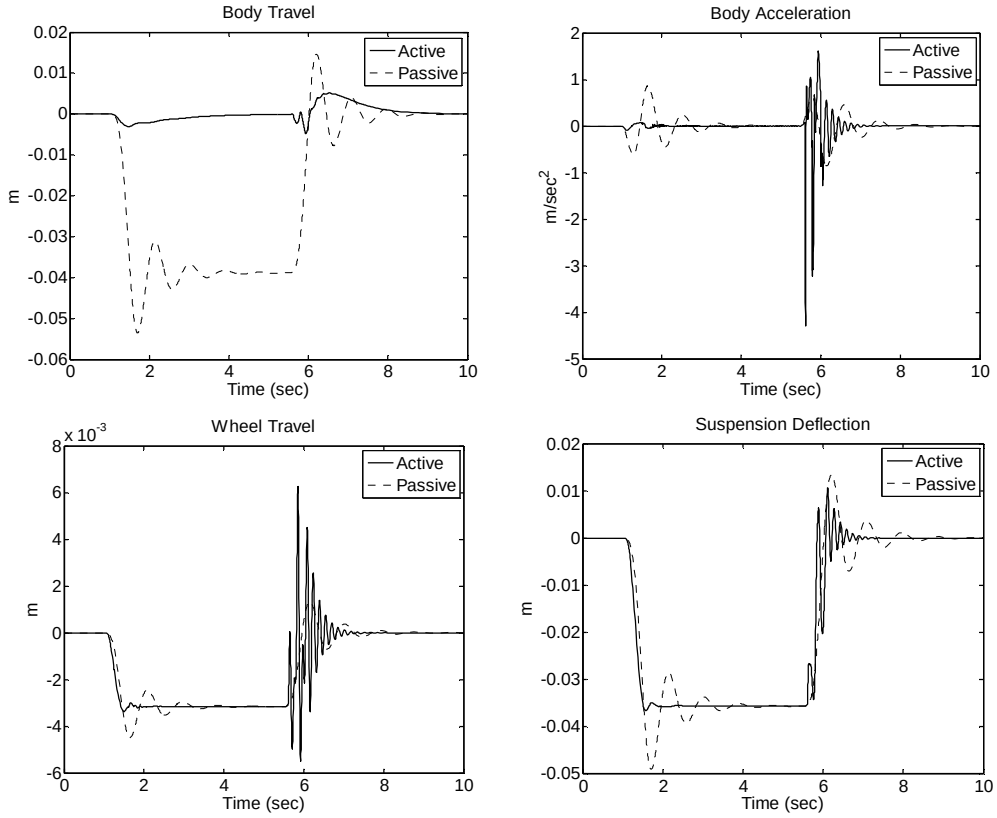

Figure (4.7): Quarter-car response of a PID with fuzzy switch control for an inertial load of 600 N.

4.2.2. Response of PID control schemes:

First we test response of PID and optimized PID controllers for road disturbances according to the function described in equation (4.2) with the use of the following control parameters to get our control laws shown in equation (3.12). For PID control, the parameters are

$$K_{sv}=0.01,\ K_p=25,\ K_i=2,\ K_d=7 \qquad (4.5)$$

And for optimized PID controller, the parameters are

$$K_{sv}=0.01,\ K_p=296.0798,\ K_i=-15.7379,\ K_d=52.0088 \qquad (4.6)$$

Figures 4.8 and 4.9 show our system response for 5 cm and 11 cm bumps, respectively with use of PID gains shown in equations (4.5) and (4.6).

Note in Fig. 4.8 that superior improvements have been reached with PID controllers with maximum body travel of 3.6mm for PID and 0.42mm for optimized PID controllers. Most importantly, acceleration has been reduced to less than 2.5m/sec^2 and less than 0.25m/sec^2 for PID and optimized PID control schemes, respectively. Also, wheel travel is good for both control schemes and suspension deflection has been reduced which will give better isolation and avoiding hitting suspension limits.

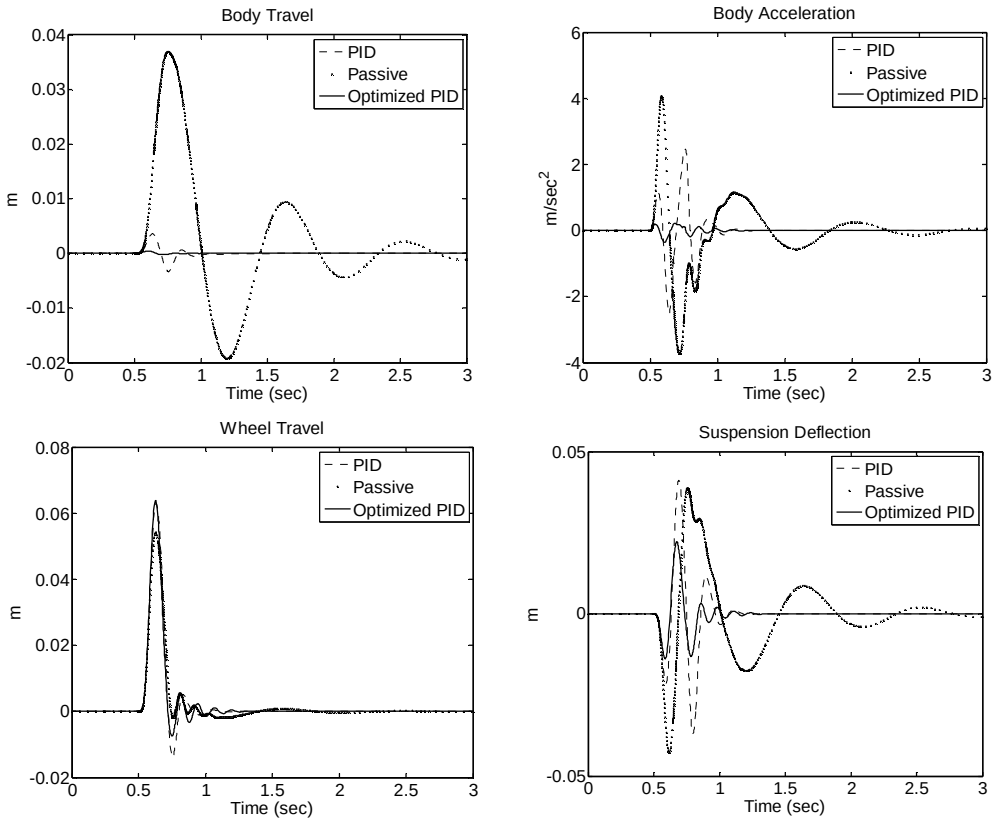

Figure (4.8): Quarter-car response of a PID control schemes for a 5 cm bump.

For an 11 cm bump, also superior improvements have been reached (see Fig. 4.9) using PID controllers with maximum body travel of 8.3mm for PID and 0.94mm for optimized PID controllers. Also, acceleration has been reduced to less than 6.25m/sec^2 and less than 0.56m/sec^2 for PID and optimized PID control schemes, respectively. This value of acceleration is notably small and forms a credited contribution for our proposed suspension. Also, wheel travel is good for both control schemes and suspension deflection has been reduced for optimized PID, but no improvements for PID control.

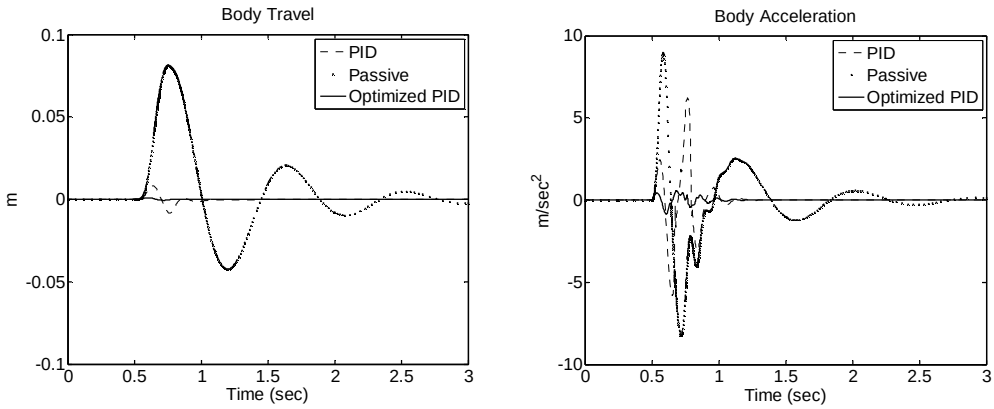

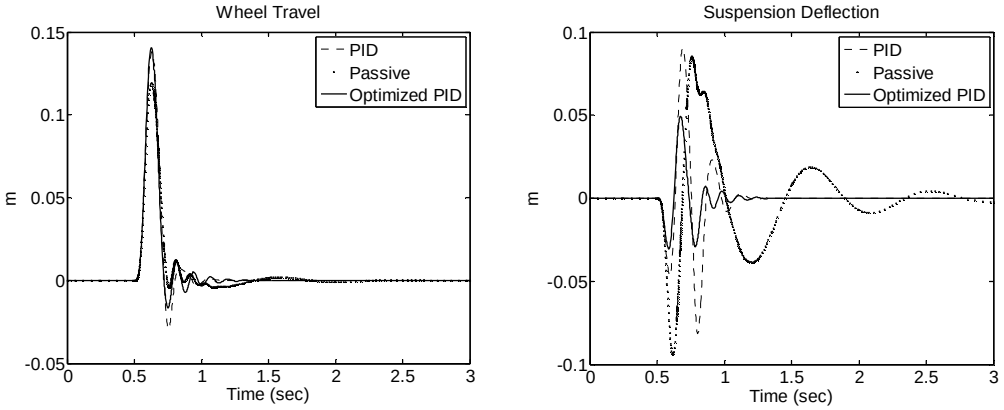

Figure (4.9): Quarter-car response of a PID control schemes for an 11 cm bump.

For inertial disturbances, response is tested similar to conditions in *Section* 4.2.1 with inertial disturbance force described in equation (4.4). Results in Fig. 4.10 have shown an excellent, fast, and very smooth response to prevent body roll. Maximum body travel is "-1 mm" for PID control and about "-0.1 mm" for optimized PID control.

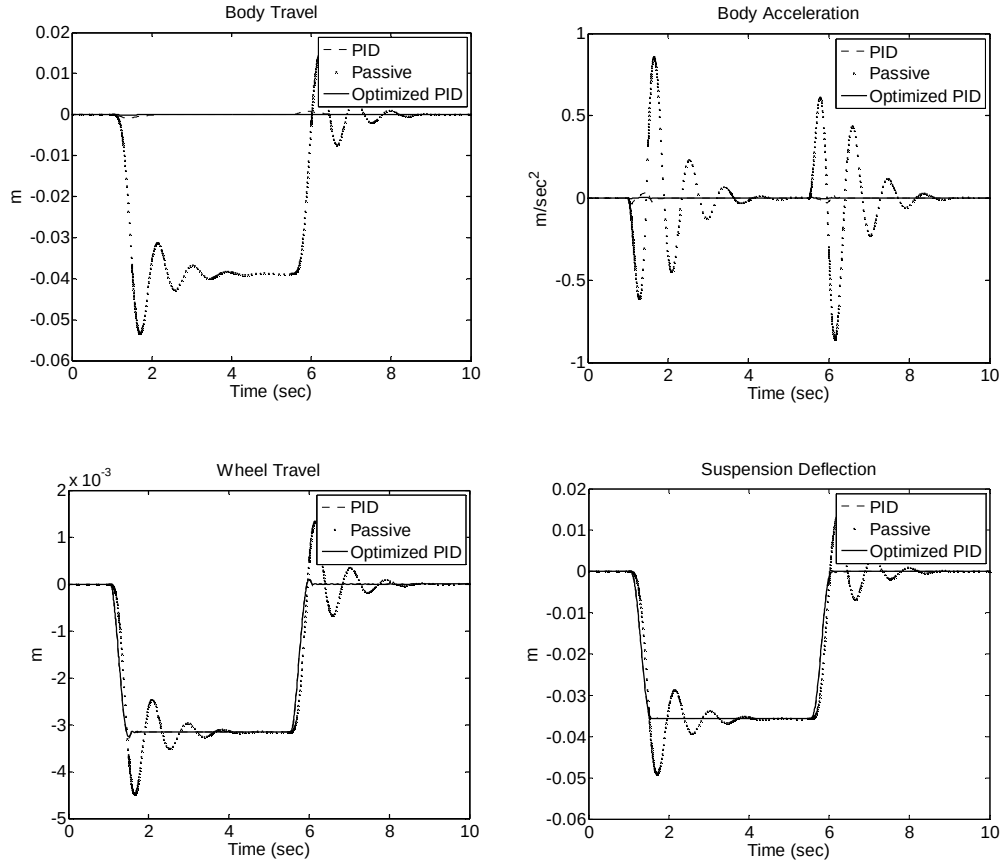

Figure (4.10): Quarter-car response of a PID control schemes for an inertial load of 600 N.

4.3. SIMULATION RESULTS FOR A HALF-CAR MODEL

Our proposed suspension with control strategies discussed in *Chapter* 3 are compared with passive suspension response for the same input. Control is applied for each quarter of the car individually. Using standard parameters and values taken from [14] and used in [5] and [7] with the half-car model parameters shown in [16]:

$$\begin{aligned} &m_c = 575\,kg, \quad m_{sf} = m_{sr} = 20\,kg, \quad m_{uf} = m_{ur}\,60\,kg, \quad c_{tf} = c_{tr} = 190000\,N/m, \\ &c_{sf} = c_{sr} = 16812\,N/m, \quad b_f = b_r = 1000\,N/m/s, \quad J_y = 769\,kg/m^2, \\ &a = 1.38\,m, \quad b = 1.36\,m, \quad \tau = 1/30\,\text{sec}, \quad P_s = 10342500\,Pa, \quad A = 3.35\times10^{-4}\,m^2, \\ &\alpha = 4.515\times10^{13}\,N/m^5, \quad \beta = 1\text{sec}^{-1}, \quad \gamma = 1.545\times10^{9}\,N/m^{5/2}kg^{1/2}. \end{aligned} \tag{4.7}$$

First we test system performance for a single road bump represented as

$$u_f(t) = \begin{cases} h(1-\cos 8\pi t), & 0.5 \le t \le 0.75 \\ 0, & otherwise \end{cases} \tag{4.8}$$

and

$$u_r(t) = \begin{cases} h(1-\cos 8\pi t), & 3 \le t \le 3.25 \\ 0, & otherwise \end{cases} \tag{4.9}$$

Note that the bump to the rear wheel is a delayed version of that of the front one.

4.3.1. Response of PID with fuzzy switch control scheme:

Bump heights are said to be 11 cm. Performance of system is compared with passive one for both the front and rear sides of the vehicle.

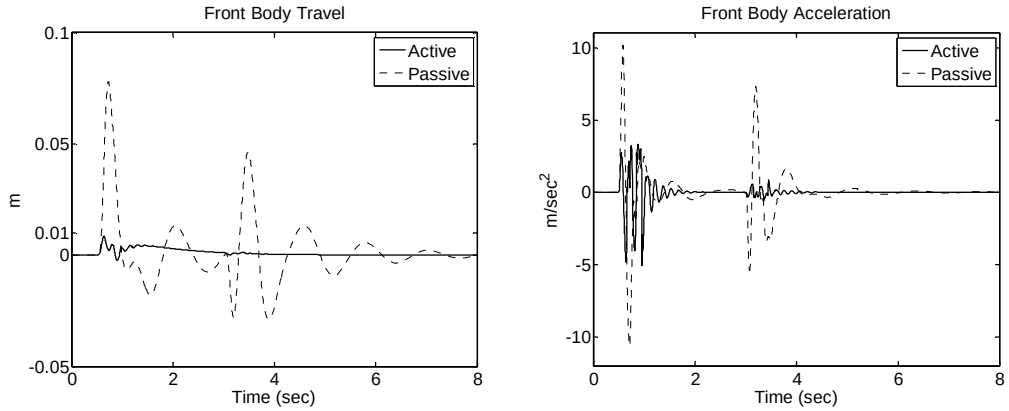

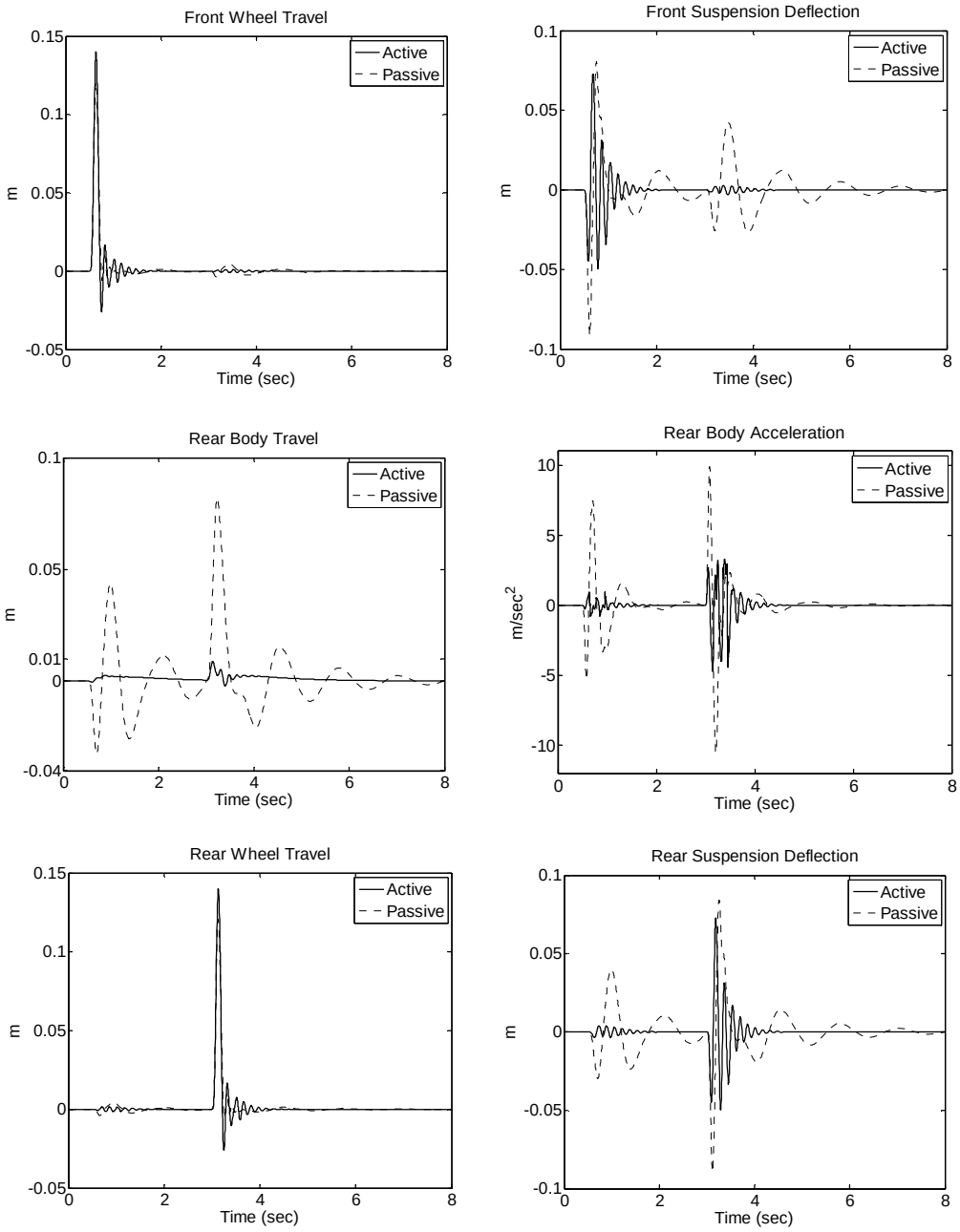

Figure (4.11): Half-car response of a PID with fuzzy switch control for an 11 cm bump.

Our proposed suspension performance is tested for inertial disturbances by applying a force to the body mass acting downwards for some time period, [10], and this force can be generated in real in the cases of cornering, braking, and accelerating. We first simulate car body cornering when inertial forces are acting on both front and rear sides of the body. Thus, inertial forces are set as follows

$$IF_f(t) = IF_r(t) = \begin{cases} 300(1-\cos 2\pi t), & 1 \le t \le 1.5 \\ 600, & 1.5 \le t \le 5.5 \\ 300(1-\cos 2\pi t), & 5.5 \le t \le 6 \\ 0, & otherwise \end{cases} \quad (4.10)$$

where *IF* stands for inertial force.

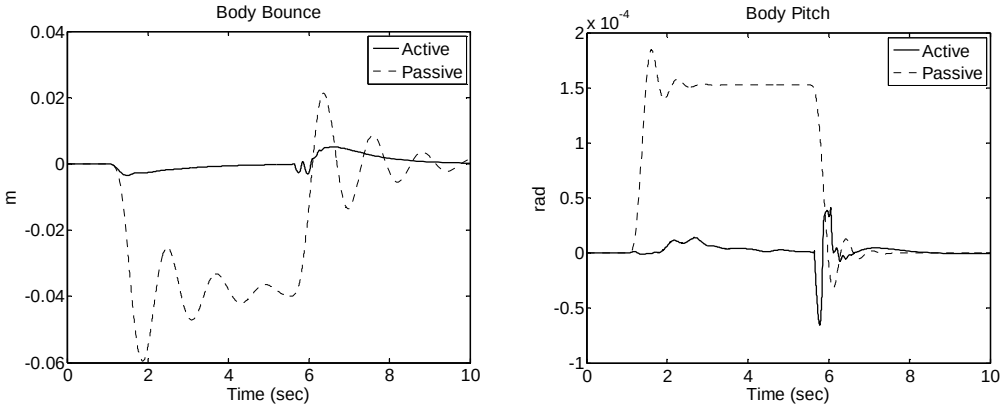

Figure (4.12): Half-car response due to inertial forces generated with car cornering situation- PID with fuzzy switch control.

Also, our proposed system with control strategy are tested for *braking* condition by applying 600N to the front side of car body, say in the period [1,6] sec, and then we simulate car *acceleration* condition where inertia force is applied to the rear side, say in the period [9,14] sec. The input forces are applied to model dynamics and are given values according to the following functions

$$IF_f(t) = \begin{cases} 300(1-\cos 2\pi t), & 1 \le t \le 1.5 \\ 600, & 1.5 \le t \le 5.5 \\ 300(1-\cos 2\pi t), & 5.5 \le t \le 6 \\ 0, & otherwise \end{cases} \quad (4.11)$$

$$IF_r(t) = \begin{cases} 300(1-\cos 2\pi t), & 9 \le t \le 9.5 \\ 600, & 9.5 \le t \le 13.5 \\ 300(1-\cos 2\pi t), & 13.5 \le t \le 14 \\ 0, & otherwise \end{cases} \quad (4.12)$$

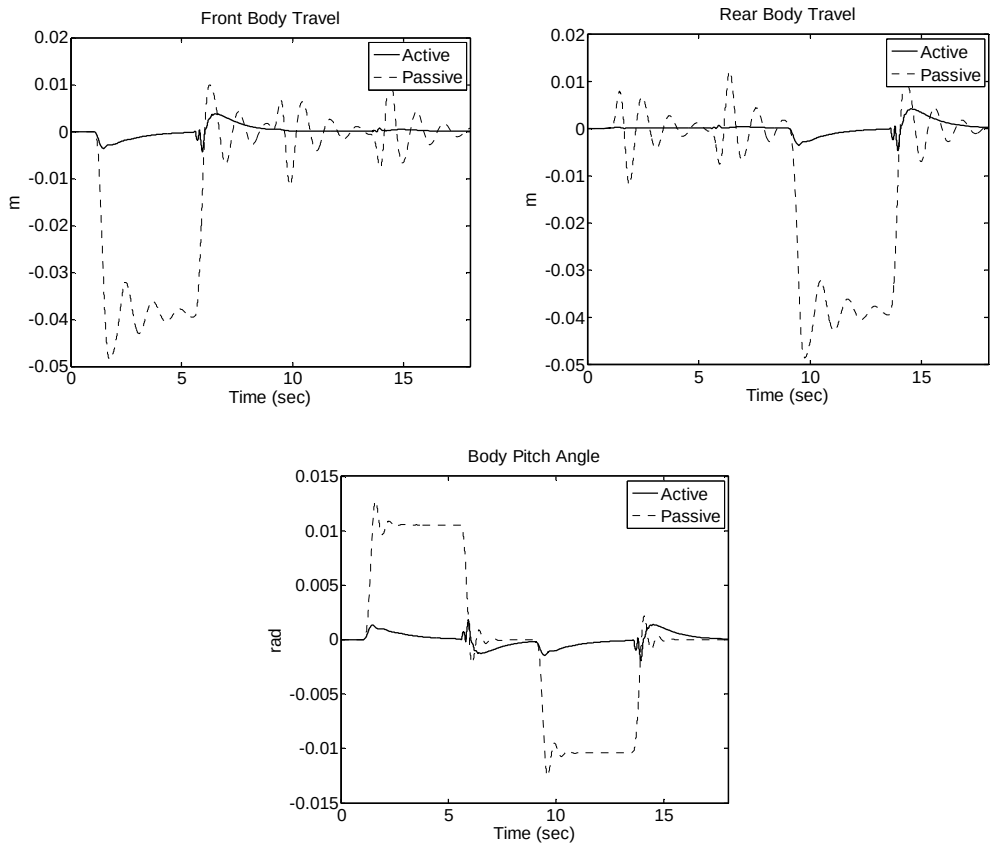

Figure (4.13): Half-car response due to inertial forces generated in car body braking(t=[1,6]sec) and acceleration(t=[9,14]sec) situations- PID with fuzzy switch control.

Results shown in Figs. 4.12 and 4.13 show good reaction for our proposed suspension structure and switching algorithm and this improved handling characteristics by preventing body roll and pitch movements.

4.3.2. Response of PID control schemes:

The same test procedure shown in the previous section is applied here with our proposed PID control schemes discussed in *Chapter* 3.

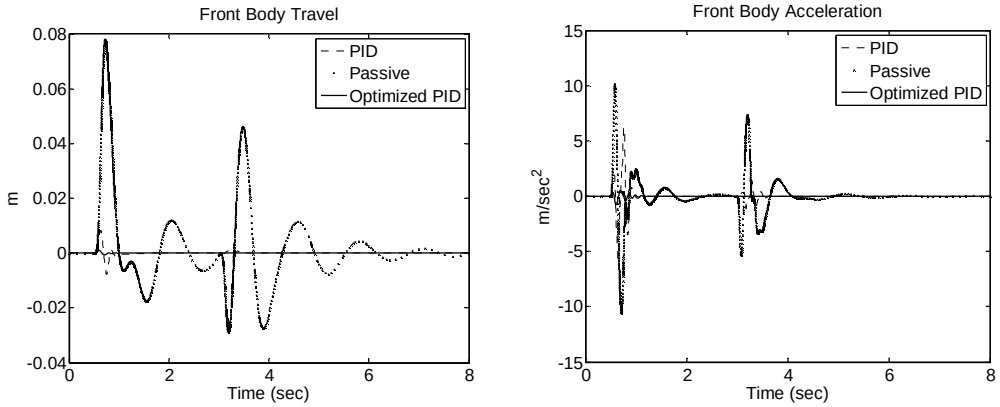

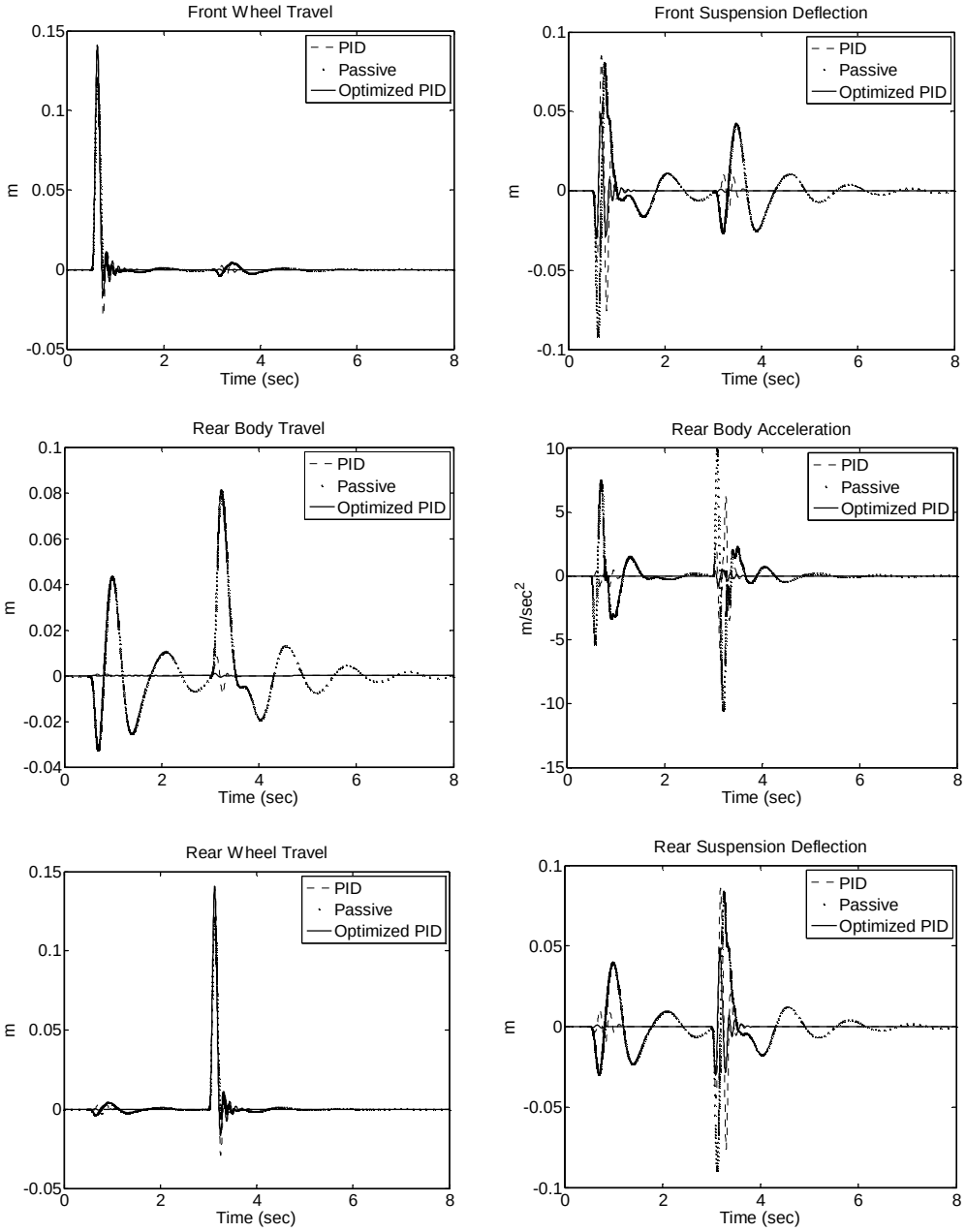

Figure (4.14): Half-car response of PID control schemes for an 11 cm bump.

When applying inertial disturbances to both front and rear sides according to equation (4.10), this simulates a cornering condition for the car. System response for this situation is shown in Fig. 4.15.

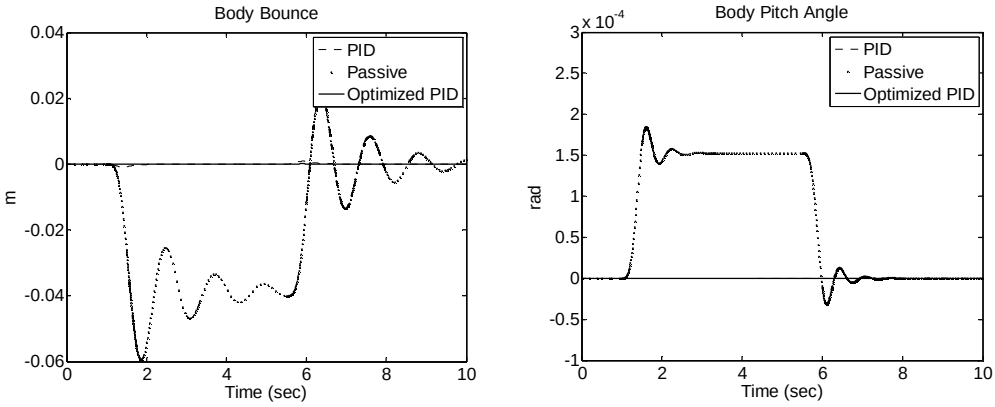

Figure (4.15): Half-car response due to inertial forces generated with car cornering situation- PID control schemes.

Note that both our PID and optimized PID controllers gave excellent response in preventing car body roll in a smooth manner. For braking and acceleration conditions, equations (4.11) and (4.12) were applied to the half-car model. Results are shown in Fig. 4.16

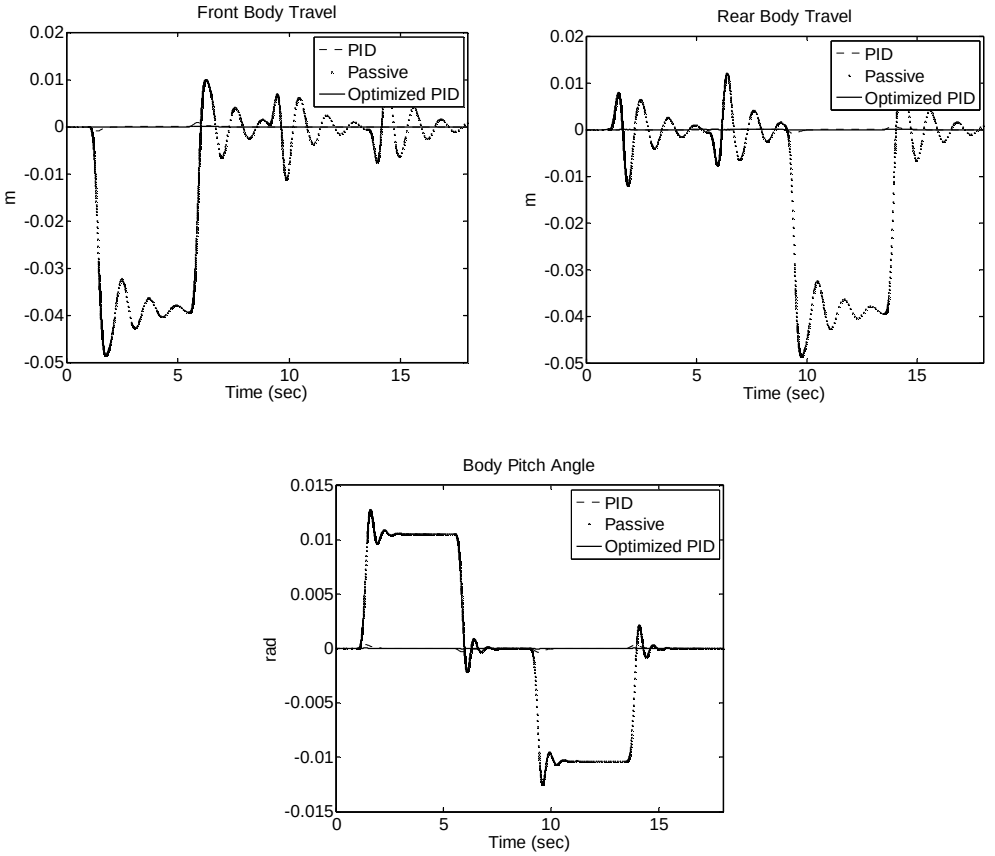

Figure (4.16): Half-car response due to inertial forces generated in car body braking(t=[1,6]sec) and acceleration(t=[9,14]sec) situations- PID control schemes.

4.4. SUMMARY OF SIMULATION RESULTS

Performance characteristics of vehicle suspensions are discussed earlier in this study and it is shown that four main characteristics are to be necessarily studied to check our improvements on suspension system. In this section we compare our control schemes performance for the same disturbances. In Fig. 4.17 maximum body travel is compared for proposed control schemes for road disturbances of 5 cm and 11 cm.

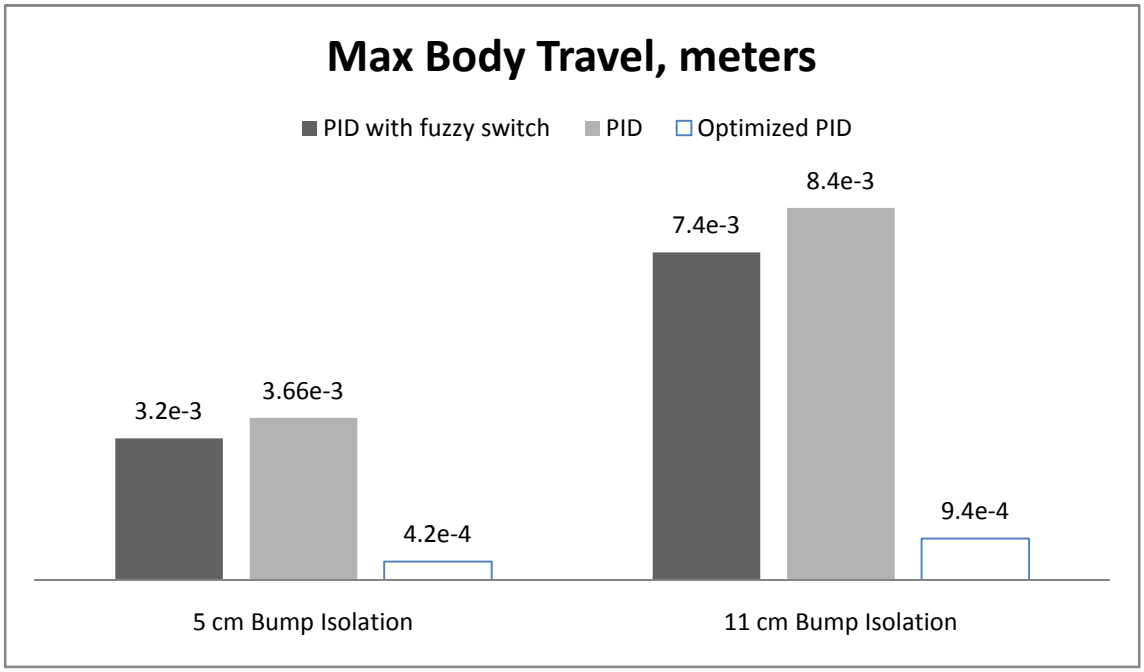

Figure (4.17): Max body travel comparison for proposed control schemes.

In Fig. 4.18, maximum positive vertical acceleration for car body is compared for our three proposed control strategies.

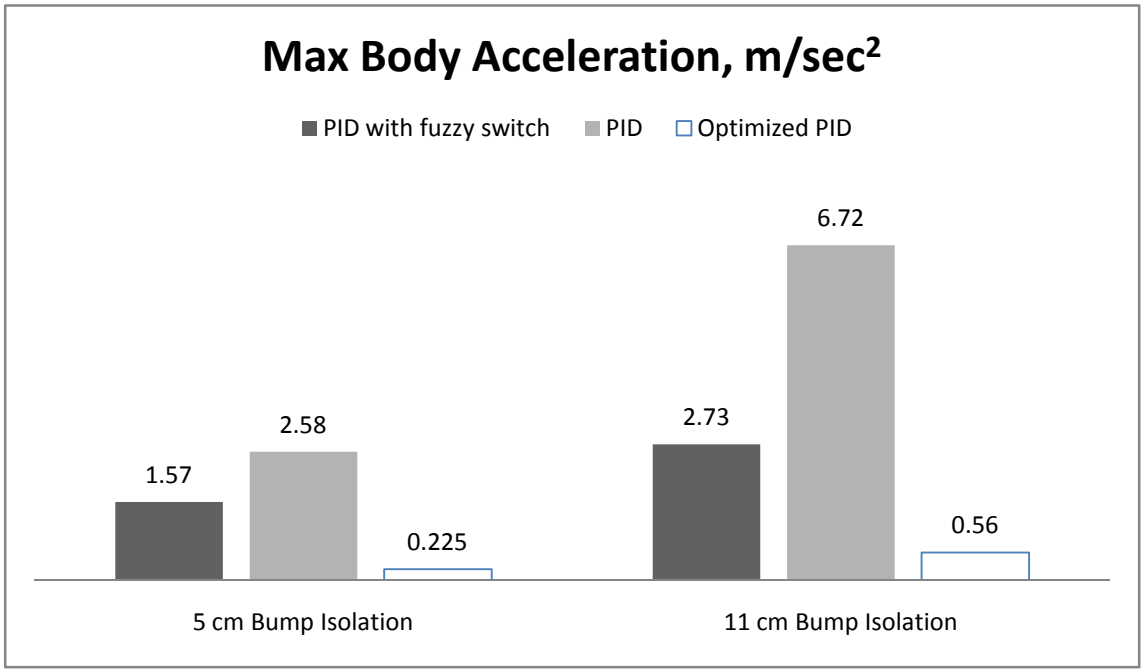

Figure (4.18): Max body acceleration comparison for proposed control schemes.

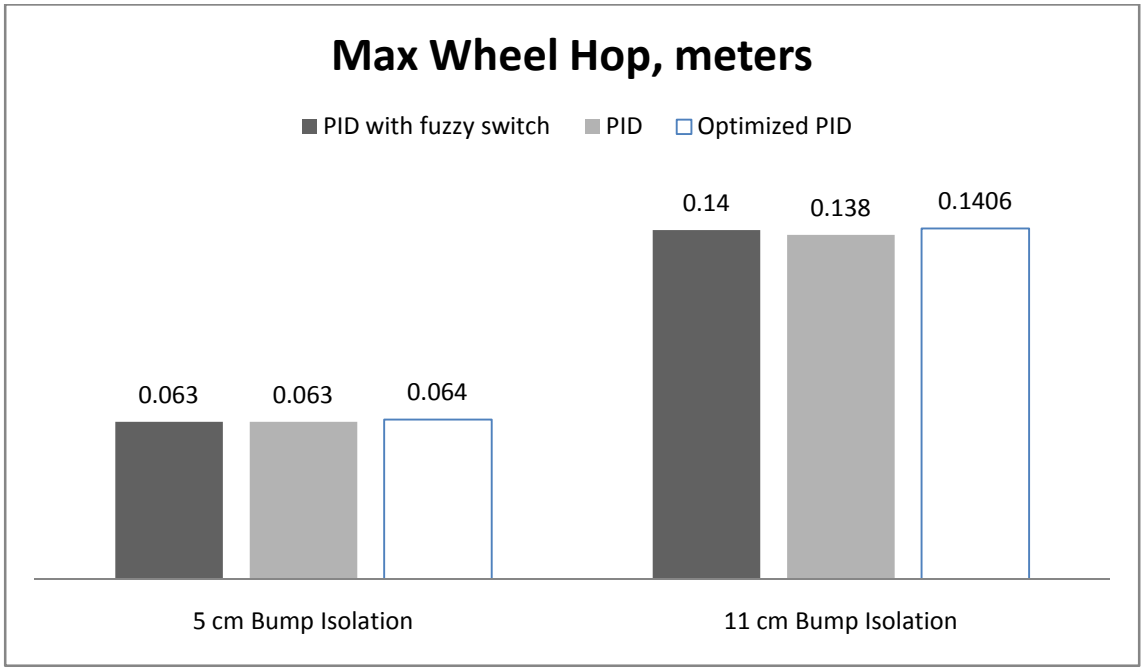

Figure (4.19): Max wheel hop comparison for proposed control schemes.

Also, a comparison of passive suspension deflection is made in order to check it is as small as possible especially when suspension deflection is negative, i.e. when the two masses are getting closer together, in order to avoid hitting suspension mechanical limits. Thus, in comparison shown in Fig. 4.20 the larger the value shown, the higher the chance to hit suspension limits and this is undesirable.

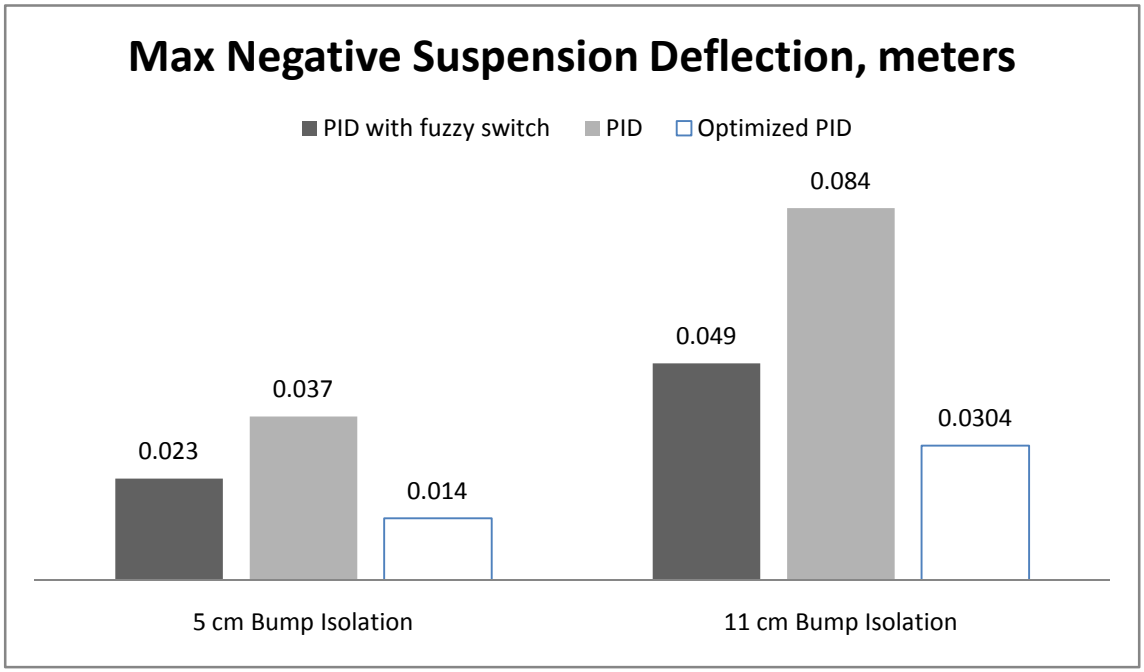

Figure (4.20): Max negative suspension deflection comparison for proposed control schemes.

4.5. COMPARISON WITH PREVIOUS STUDIES FOR QUARTER-CAR

Proposed suspension system in this study forms a special assembly that can be classified as a low-bandwidth suspension system. This resulted in a satifactory a low frequency control with linear controllers. However, results obtained have shown excellent performance for the suspension in addition to the expected decrease in system energy requirements due to low frequency operating range of the actuator, [8]. In this section we show a comparison between results of this study with previous studies results in achieving desired performance characteristics concerning vehicle ride and comfort. Most of previous studies do not include system response for inertial loads. Thus, comparison will be only for system bump isolation.

Results of two previous studies are shown below in a comparison with the results got by our optimized PID control; first study was made by Lin, J.-S. and Kanellakopoulos, I. in 1997, [5] and introduced a nonlinear backstepping control to a high-bandwidth active suspension, the other study was made by Fialho, I. and Balas, G. in 2002, [7] and introduced an adaptive control strategy applied to high bandwidth active suspensions. The two studies employed full nonlinear dynamics of the hydraulic actuator and with the same system parameters used in this study.

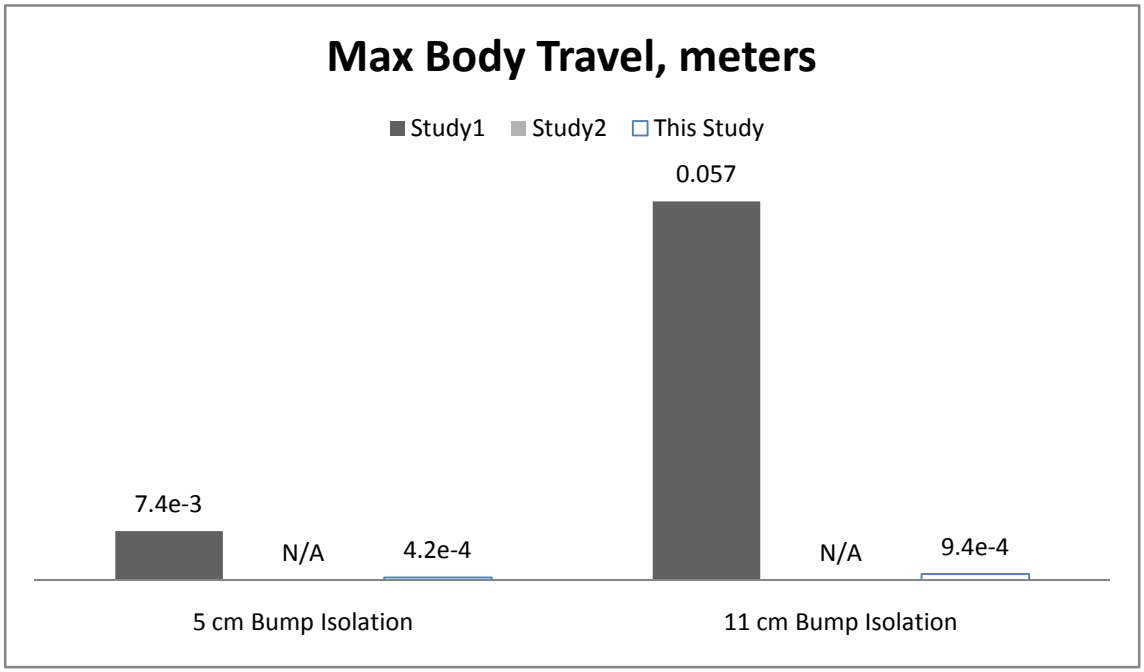

Figure (4.21): Max body travel comparison with previous studies.

In Fig. 4.21, achieved reduction in car body travel by our system is excellent compared with results obtained in [5]. N/A stands for (Not Available).

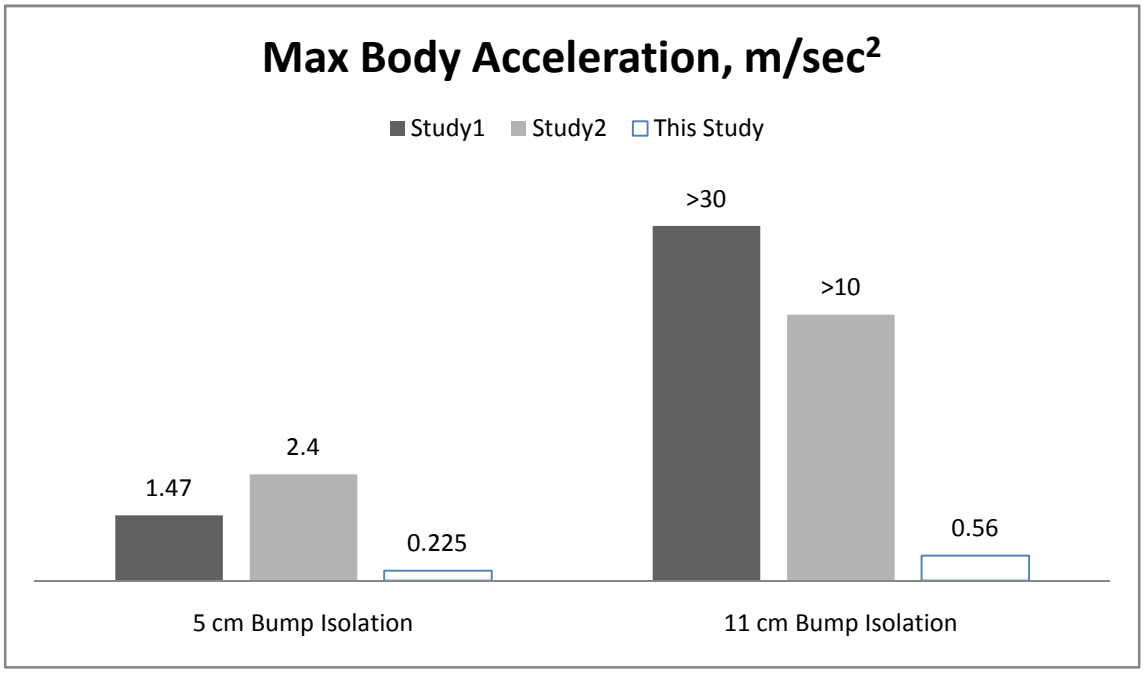

Figure (4.22): Max body acceleration comparison with previous studies.

Superior performance of our proposed system is shown clearly in acceleration level shown in Fig. 4.22.

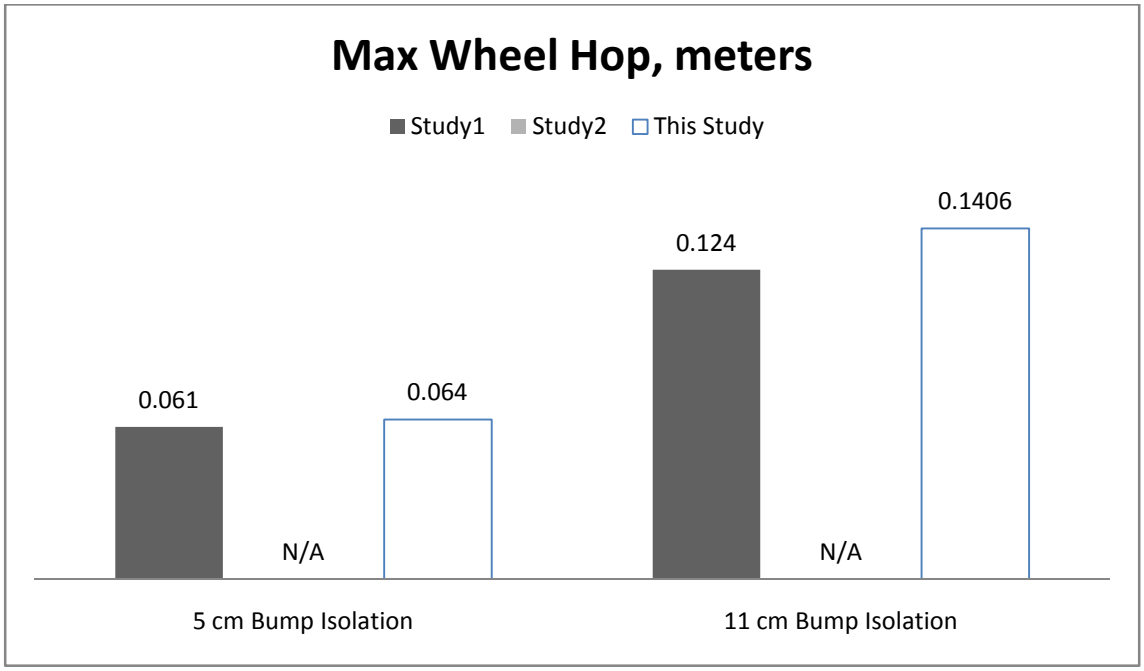

Figure (4.23): Max wheel hop comparison with previous studies.

Our system has no improvements regarding wheel hop over passive suspension as mentioned earlier throughout this study.

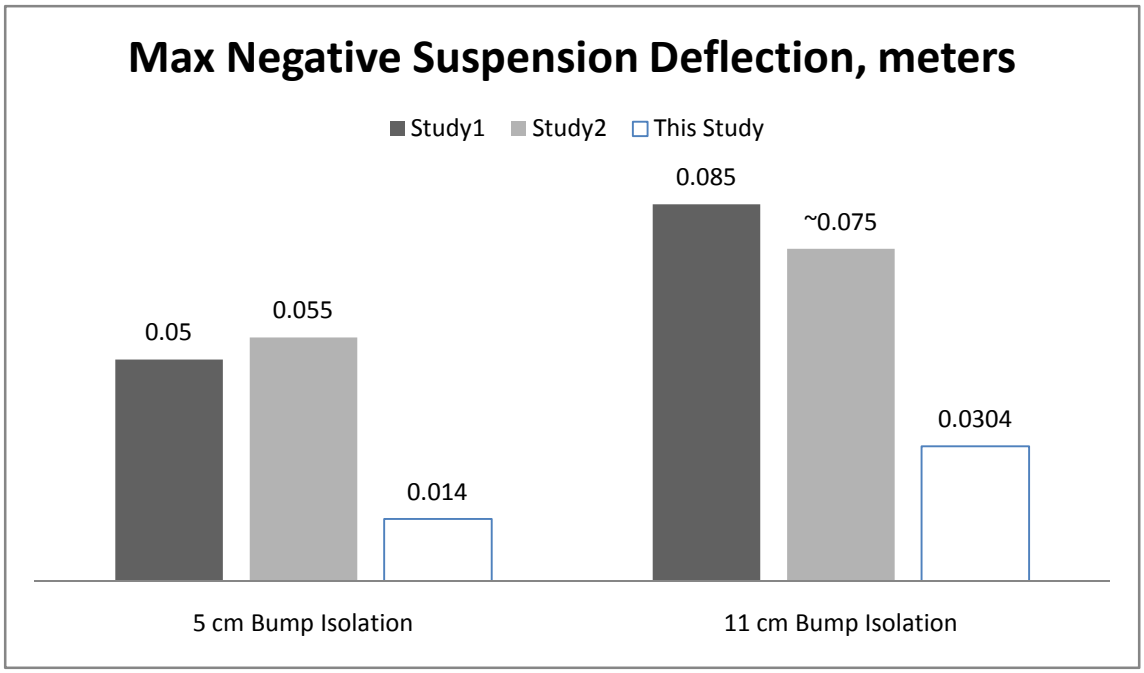

Figure (4.24): Max negative suspension deflection comparison with previous studies.

4.6. POWER REQUIREMENTS AND ENERGY CONSUMPTIONS

In this section we show a comparison between our three proposed control schemes regarding power requirements and energy consumption for each case. Comparison is made to quarter car model with applying road disturbance of an 11 cm height bump according to equation (4.2) and then for an inertial load acording to equation (4.4).

Power requirements for each of the three control schemes, PID with fuzzy switch, PID, and optimized PID, is calculated using equation (3.26) and energy consumed in bump isolation is calculated applying equation (3.28).

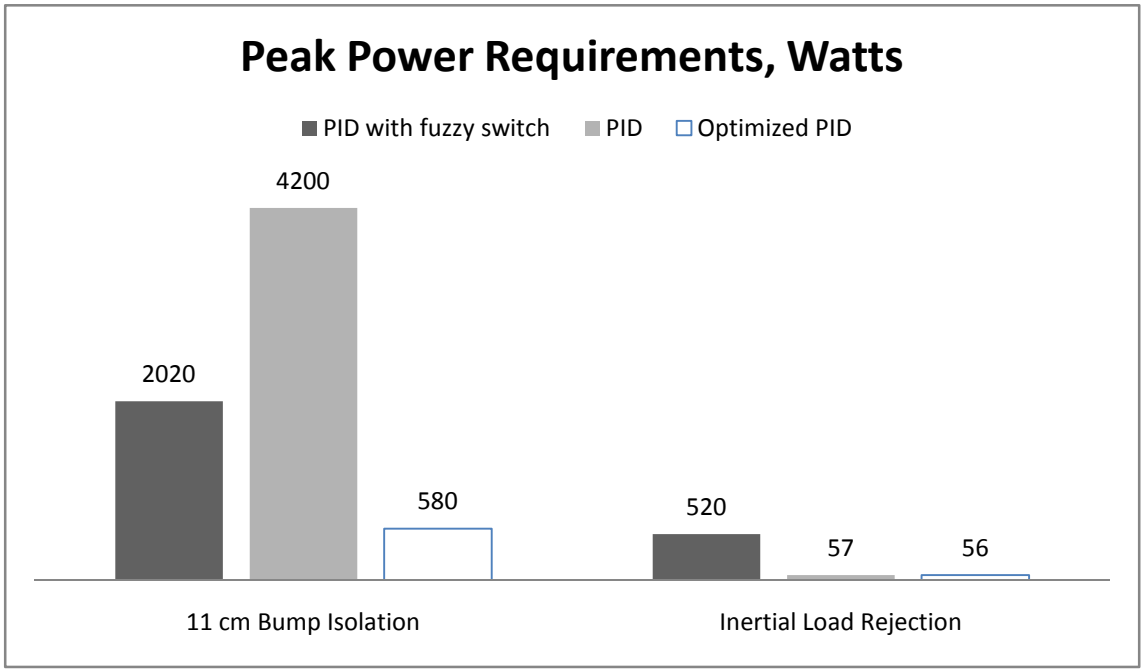

Figure (4.25): Peak power requirements for our different control strategies for bump isolation and inertial load compensation cases.

Note that optimized PID control has excellent specifications in power requirements. Also, PID with fuzzy switch control is better than PID control for bump rejection. Furthermore, note the high value of power requirement of PID with fuzzy switch scheme due to its undesirable response for inertial load release situation.

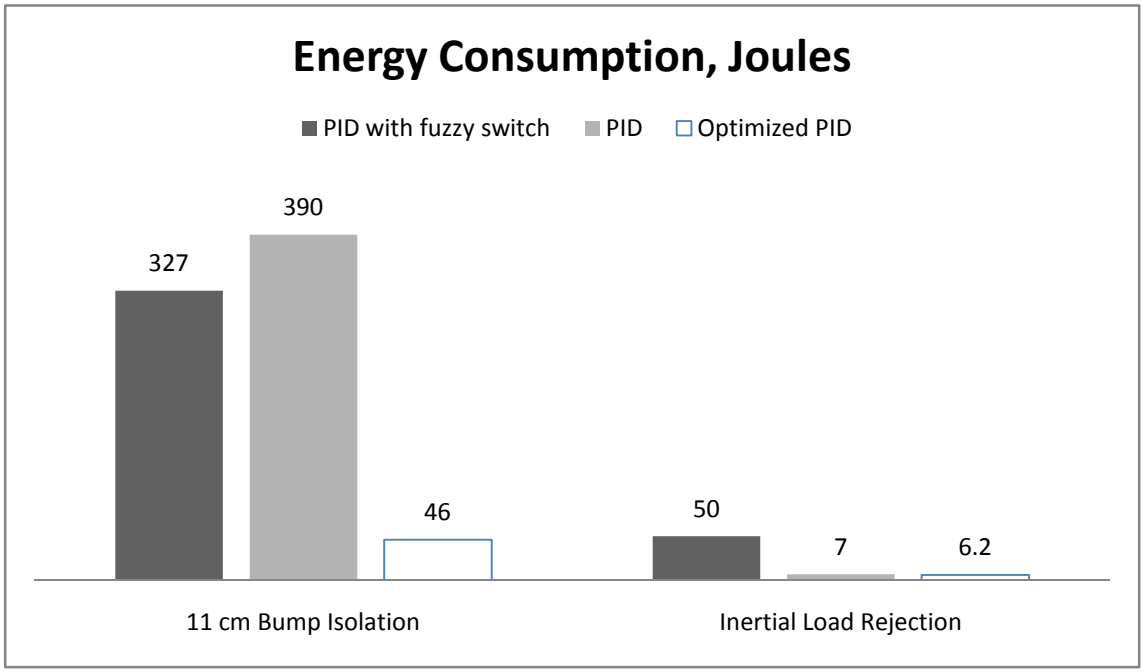

Figure (4.26): Energy consumptions for our different control strategies for bump isolation and inertial load compensation cases.

5. CONCLUSION AND FUTURE WORK

5.1. CONCLUSION

In this study a special construction of low bandwidth active suspensions was introduced with three control schemes. The first employed a PID control with fuzzy algorithm to switch between two control objectives; bump rejection and inertial load rejection. The second employed PID control which has been tuned by trial and error and the third employed an optimized PID control in which parameters were tuned to achieve some constraints in output response. Proposed system with control schemes had shown superior response in bump isolation and inertial disturbances rejection and had a notable improvement in ride comfort characteristic of the suspension especially for the optimized PID scheme as it lowered maximum body acceleration by 94.3% and reduced body travel by 98.8% of that of passive one.. The proposed system and controllers had no improvements regarding wheel hop over passive suspensions, but handling characteristic still acceptable.

Power requirements of proposed suspension were discussed and calculated throughout the study in addition to energy consumptions for each of the three proposed control schemes. Optimized PID control had shown lower power needs.

Control strategies introduced in this study were also applied to a half-car model to test mutual reactions between front and rear sides of the vehicle and our control strategies showed superior performance in ride quality over passive suspension.

5.2. RECOMMENDED FUTURE WORK

Improvements should be made to the fuzzy switch introduced in our first control strategy in order to overcome the problem of the unwanted vibrations occurs when inertial disturbance is released. On the other hand, optimal techniques may be employed in order to reduce the value of the sprung mass. Also, nonlinear and

adaptive techniques may be employed to improve response of the actuator by adapting nonlinear characteristics of the system and switching between operating conditions. This may also improve system response in the presence of uncertainties.

REFERENCES

[1] Appleyard, M.; Wellstead, P.E.: *Active Suspensions: some background*, IEE Proc. of Control Theory Appl., Vol. 142, No. 2, pp. 123-128, (1995).

[2] Gillespie, T.D.: *"Fundamentals of Vehicle Dynamics"*, SAE International, (1992).

[3] Williams, R.A.: *Automotive active suspensions*, Jaguar Cars, Coventry, England, (1994).

[4] Williams, R.A.: *Electronically controlled automotive suspensions*, Computing & Control Engineering Journal, pp. 143-148, June, (1994).

[5] Lin J.S.; Kanellakopoulos, I.: *Nonlinear design of active suspensions*, Control System Magazine, Vol. 17, pp. 45–59, (1997).

[6] Williams, R.A.; Best, A.: *Control of a low frequency active suspension*, IEE Control Conf., No. 389, (March, 1994).

[7] Fialho, I.; Balas, G.J.: *Road adaptive active suspension design using linear parameter-varying gain-scheduling*, IEEE Transactions on Control Systems Technology, Vol. 10, No. 1, (January, 2002).

[8] Shuttlewood, D.W.; Crolla, D.A.; Sharp, R.S.: *Theoretical results of an electrically actuated hydro-pneumatic slow-active suspension*, IFToMh4-j c International Symposium on Theory of Machines and Mechanisms, Nagoya, Japan, (September, 1992).

[9] Truscott, A.J.; Burton, A.W.: *On the analysis, modeling and control of an advanced suspension system*, IEE Control Conference, No. 389, pp. 183-189, (March, 1994).

[10] Truscott, A.J.: *Composite active suspension for automotive vehicles*, Computing & Control Engineering Journal, pp. 149-154, (1994).

[11] Burton, A.W.; Truscott, A.J.; Wellstead, P.E.: *Analysis, modelling and control of an advanced automotive self-levelling suspension system*, IEE Proc. of Control Theory Appl., Vol. 142, No. 2, pp. 129-139, (March, 1995).

[12] Webb, A.C.; Burnham, K.J.; James D.J.G.; Williams, R.A.: *Adaptive control of a low bandwidth active suspension system*, UKACC International Conference on Control, No. 427, pp. 1154-1159, (September, 1996).

[13] Merritt, H.E.: *"Hydraulic Control Systems"*, New York, NY: John Wiley & Sons, (1967).

[14] Alleyne, A.; Hedrick, J.K.: *Nonlinear control of a quarter car active suspension*, Proceedings of the American Control Conference, Chicago IL, pp. 21–25, (1992).

[15] Alleyne, A.; Hedrick, J.K.: *Nonlinear adaptive control of active suspensions*, IEEE Transactions on Control System Technology, Vol. 3, No. 1, pp. 94-101, (March, 1995).

[16] Lin, J.S.; Huang, C.J.: *Nonlinear backstepping active suspension design applied to a half-car model*, Vehicle System Dynamics, Vol. 42, No. 6, pp. 373-393, (2004).

[17] Sam, Y.; Osman, J.H.S.; A.Ghani, M.R.: *Sliding mode control of active suspension system*, Jurnal Teknologi, No. 37(D), pp. 1-10, UTM, (2002).

[18] Sam. Y.; Osman, J.H.S.*: Modeling and control of the active suspension system using proportional integral sliding mode approach*, Asian Journal of Control, Vol. 7, No. 2, pp. 91-98, (June, 2005).

[19] Sam, Y.; Osman, J.H.S.: *Sliding mode control of a hydraulically actuated active suspension*, Jurnal Teknologi, No. 44(D), pp. 37-48, UTM, (June, 2006).

[20] Sam, Y.; Hudha, K.: *PI/PISMC control of hydraulically actuated active suspension system*, Proc. of 1st Regional Conf. on Vehicle Engineering and Technology, Kuala Lumpur, (July, 2006).

[21] Miaomiao, M.; Hong, C.; Yanfeng, C.: *Backstepping based constrained control of nonlinear hydraulic active suspensions*, Proc. of the 26th Chinese Control Conference, China, (2007).

[22] Basari, A.A.; Saat, M. S.: *Control of a quarter car nonlinear suspension system*, IEEE, Asia-Pacific Conf. on Applied Electromagnetic Proc., Melaka, Malaysia, (December, 2007).

[23] Sam, Y.; Suaib, N.M; Osman, J.H.S.: *Proportional integral sliding mode control for half-car active suspension system with hydraulic actuator*, 8th WSEAS Conf. (ROCOM), pp. 52-57, China, (2008).

[24] Hashemipour, H.; Amiri, M.; Mirzaei, M.; Maghoul, A.: *Nonlinear control of vehicle active suspension considering actuator dynamics*, IEEE Second ICCEE, pp. 362-366, (2009).

[25] Hassanzadeh, I.; Alizadeh, G.; Shirjoposht, N.P.; Hashemzadeh, F.: *A new optimal nonlinear approach to half car active suspension control*, IACSIT International Journal of Engineering and Technology Vol. 2, No.1, pp. 78-84, ISSN: 1793-8236, (February, 2010).

[26] Ekoru, J.E.D.; Dahunsi, O.A.; Pedro, J. O.: *PID control of a nonlinear half-car suspension system via force feedback*, IEEE Africon, Zambia, (2011).

[27] Kaddissi, C.; Kenné, J.P.; Saad, M.: *Drive by wire control of an electro-hydraulic active suspension a backstepping approach*, IEEE Conference on Control Applications, pp. 1581-1587, Canada, (August, 2005).

[28] Sam, Y.: *Robust control of active suspension system for a quarter car model*, UTM, (2006).

[29] Chung, J.S.: *Analysis of series type and parallel type active suspensions*, pp. 177-182, Hsinchu, Taiwan, (November, 2007).

[30] Kumar, M.S.; Vijayaragan, S.: *Analytical and experimental studies on active suspension system of light passenger vehicle to improve ride comfort*, Mechanika, ISSN 1392-1207, No. 3 (65), pp. 34-41, (2007).

[31] Lin, J.S.; Kanellakopoulos, I.: *Road-adaptive nonlinear design of active suspensions*, Proc. of the American Control Conference, pp. 714-718, (June, 1997).

[32] Zulfatman: *Identification of test rig for a quarter car active suspension systems*, M.Sc. Thesis, UTM, (2008).

[33] Çetin, Ş.; Demir, Ö.: *Fuzzy PID controller with coupled rules for a nonlinear quarter car model*, World Academy of Science, Engineering and Technology (41), pp. 238-241, (2008).

[34] Gordon, T. J.; Best, M. C.: *Dynamic optimization of nonlinear semi-active suspension controllers*, IEE Control Conference, No. 389, pp. 332-337, (1994).

[35] Chantranuwathana, S.; Peng, H.: *Adaptive robust control for active suspensions*, Proc. of the American Control Conference, pp. 1702-1706, (June, 1999).

[36] Yagiz, N.; Sakman, L.; Guclu, R.: *Different control applications on a vehicle using fuzzy logic control*, *S¯adhan¯a*, Vol. 33, Part 1, pp. 15-25, (February, 2008).

[37] Burns, R.S.: *"Advanced Control Engineering"*, Butterworth-Heinemann, Linacre House, Jordan Hill, Oxford, (2001).

[38] Ogata, K.: *"Modern Control Engineering"*, 4th ed., Prentice Hall, Upper Saddle River, N.J., (2002).

[39] Dorf, R.C.; Bishop, R.H.: *"Modern Control Systems"*, 10th ed., Prentice Hall, Upper Saddle River, NJ 07458, (2005).

[40] Wong, A.L.: *Axiomatic design of a customizable pneumatic automotive suspension with hydraulic ride height regulator*, B. Sc. Mechanical Engineering Thesis, MIT, (May, 2005).

APPENDIX

This appendix shows setup and main blocks built in the MATLAB and SIMULINK environments to simulate passive quarter car introduced throughout this study. Also, m-file code set to visualize comparison animation between our active suspension and passive one is shown.

A.1. PASSIVE QUARTER CAR MODEL

Passive suspension is shown in Fig. 1.1 (a) and mathematical model can be written as

$$\begin{aligned} \ddot{x}_{us} &= \frac{1}{m_{us}}[c_2(x_s - x_{us}) + b(\dot{x}_s - \dot{x}_{us}) - c_1(x_{us} - u)] \\ \ddot{x}_s &= \frac{1}{m_s}[-c_2(x_s - x_{us}) - b(\dot{x}_s - \dot{x}_{us})] \end{aligned} \tag{A.1}$$

Model built for our study is shown in Fig. A.1.1

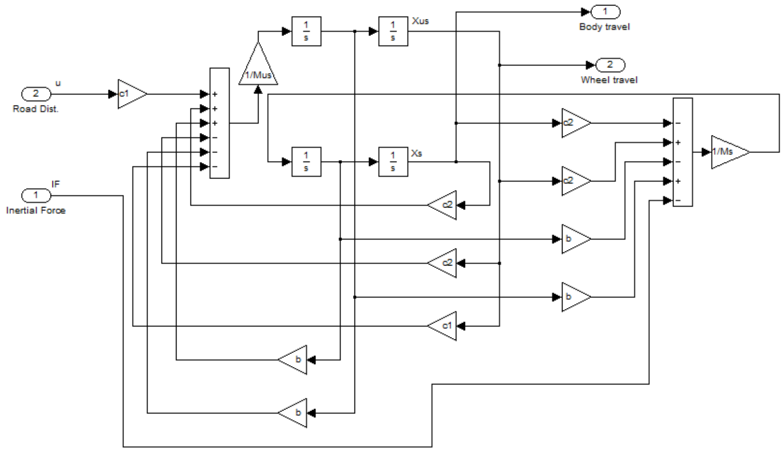

Figure (A.1.1): Passive suspension SIMULINK model.

A.2. M-FILE CODE TO VISUALIZE SYSTEM RESPONSE

Simulations outputs for our system are saved to MATLAB workspace in the format: *Structure with time* and these data are called in our m-file code

```
%                       Car Animation Script
%
% This Matlab script is used in conjunction with our Simulink model to
% produce an animation of the quarter-car body response for different
% road and inertial disturbances.
%
%%%%%            Done by: Mohammad Hafez F. AbuShaban
%%%%%                  within M.Sc. thesis
%
% The script assumes your Simulink model has created the following vectors
% related to the motion of the quarter-car model:
% {y_b1a} is the structure with passive suspension body travel
% {y_b3a} is the structure with active suspension body travel
% {y_w1a} is the structure with passive suspension wheel travel
% {y_w3a} is the structure with active suspension body travel
% {y_sa} is the structure with active suspension disc travel
% {y_r} is the structure with road disturbance value
% {FF} is the structure with inertial force disturbance

% Paramter Setup for Car Animation
dxb=0.5;yb0=1.75;dyb=0.25; % Define quarter-car body chassis mass dimensions
yw0=0; % Define wheel dimensions


y_b1=(y_b1a.signals.values);
y_b3=(y_b3a.signals.values);
y_w1=(y_w1a.signals.values);
y_w3=(y_w3a.signals.values);
y_s=(y_sa.signals.values);
y_r=(y_ra.signals.values);
F=(FF.signals.values);

%%% Clear the workshop screen
clc;
y_cy3=y_b3;
length(y_b1)
%%% Enter Loop to Create Car Animation
for i = 1:30:length(y_b1)
figure(1);clf(1)

if F(i)>0
    plot([-1-0.15,-1],[y_b1(i)+yb0+dyb+0.2,y_b1(i)+yb0+dyb],'k-','MarkerSize',5,'linewidth',2);hold on
    plot([-1,-1+0.15],[y_b1(i)+yb0+dyb,y_b1(i)+yb0+dyb+0.2],'k-','MarkerSize',5,'linewidth',2);
    plot([-1-0.15,-1-0.08],[y_b1(i)+yb0+dyb+0.2,y_b1(i)+yb0+dyb+0.2],'k-','MarkerSize',5,'linewidth',2);
    plot([-1+0.08,-1+0.15],[y_b1(i)+yb0+dyb+0.2,y_b1(i)+yb0+dyb+0.2],'k-','MarkerSize',5,'linewidth',2);
    plot([-1.08,-1.08],[y_b1(i)+yb0+dyb+0.4,y_b1(i)+yb0+dyb+0.2],'k-','MarkerSize',5,'linewidth',2);
    plot([-1+0.08,-1+0.08],[y_b1(i)+yb0+dyb+0.4,y_b1(i)+yb0+dyb+0.2],'k-','MarkerSize',5,'linewidth',2);
    plot([-1-0.08,-1+0.08],[y_b1(i)+yb0+dyb+0.4,y_b1(i)+yb0+dyb+0.4],'k-','MarkerSize',5,'linewidth',2);
    plot([1-0.15,1],[y_b3(i)+yb0+dyb+0.2,y_b3(i)+yb0+dyb],'k-','MarkerSize',5,'linewidth',2);
    plot([1+0.15,1],[y_b3(i)+yb0+dyb+0.2,y_b3(i)+yb0+dyb],'k-','MarkerSize',5,'linewidth',2);
    plot([1-0.15,1-0.08],[y_b3(i)+yb0+dyb+0.2,y_b3(i)+yb0+dyb+0.2],'k-','MarkerSize',5,'linewidth',2);
    plot([1+0.08,1+0.15],[y_b3(i)+yb0+dyb+0.2,y_b3(i)+yb0+dyb+0.2],'k-','MarkerSize',5,'linewidth',2);
    plot([1.08,1.08],[y_b3(i)+yb0+dyb+0.4,y_b3(i)+yb0+dyb+0.2],'k-','MarkerSize',5,'linewidth',2);
    plot([1-0.08,1-0.08],[y_b3(i)+yb0+dyb+0.4,y_b3(i)+yb0+dyb+0.2],'k-','MarkerSize',5,'linewidth',2);
    plot([1-0.08,1+0.08],[y_b3(i)+yb0+dyb+0.4,y_b3(i)+yb0+dyb+0.4],'k-','MarkerSize',5,'linewidth',2);
end
%%%%%%%%%%%%%%%%%%%%%%%%%%%%%%%%%%%%%%%%%%%%%%%%%%%%%%%%%%%%%%%%%%%%%%%%%%%%%%
```

APPENDIX

```
%%%%%%%%%%%%%%%%          Passive Suspension       %%%%%%%%%%%%%%%%%%%%%%%%%%
%%% Draw Car Body
x=[-1+dxb, -1+dxb, -1-dxb, -1-dxb];
y=[y_b1(i)+yb0+dyb, y_b1(i)+yb0-dyb, y_b1(i)+yb0-dyb, y_b1(i)+yb0+dyb];
patch(x,y,'r'); hold on;
%%% Draw Wheel
t = 0:pi/20:2*pi;
patch(0.43*sin(t)-1,0.43*cos(t)+y_w1(i),'k')
patch(0.281*sin(t)-1,0.281*cos(t)+y_w1(i),'w')
%%% Draw Conventional Spring and Damper Connecting Sprung mass to Wheel
plot([-1,-1-0.15],[y_b1(i)+yb0,y_b1(i)+yb0-((y_b1(i)+yb0-y_w1(i)-yw0)/40)],'g-','MarkerSize',5,...
    'linewidth',3);
plot([-1+0.15,-1-0.15],[y_b1(i)+yb0-3*((y_b1(i)+yb0-y_w1(i)-yw0)/40),y_b1(i)+yb0-5*((y_b1(i)+yb0...
    -y_w1(i)-yw0)/40)],'g-','MarkerSize',5,'linewidth',3);
plot([-1+0.15,-1-0.15],[y_b1(i)+yb0-7*((y_b1(i)+yb0-y_w1(i)-yw0)/40),y_b1(i)+yb0-9*((y_b1(i)+yb0...
    -y_w1(i)-yw0)/40)],'g-','MarkerSize',5,'linewidth',3);
plot([-1+0.15,-1-0.15],[y_b1(i)+yb0-11*((y_b1(i)+yb0-y_w1(i)-yw0)/40),y_b1(i)+yb0-13*((y_b1(i)+yb0...
    -y_w1(i)-yw0)/40)],'g-','MarkerSize',5,'linewidth',3);
plot([-1+0.15,-1-0.15],[y_b1(i)+yb0-15*((y_b1(i)+yb0-y_w1(i)-yw0)/40),y_b1(i)+yb0-17*((y_b1(i)+yb0...
    -y_w1(i)-yw0)/40)],'g-','MarkerSize',5,'linewidth',3);
plot([-1+0.15,-1-0.15],[y_b1(i)+yb0-19*((y_b1(i)+yb0-y_w1(i)-yw0)/40),y_b1(i)+yb0-21*((y_b1(i)+yb0...
    -y_w1(i)-yw0)/40)],'g-','MarkerSize',5,'linewidth',3);
plot([-1+0.15,-1-0.15],[y_b1(i)+yb0-23*((y_b1(i)+yb0-y_w1(i)-yw0)/40),y_b1(i)+yb0-25*((y_b1(i)+yb0...
    -y_w1(i)-yw0)/40)],'g-','MarkerSize',5,'linewidth',3);
plot([-1+0.15,-1-0.15],[y_b1(i)+yb0-27*((y_b1(i)+yb0-y_w1(i)-yw0)/40),y_b1(i)+yb0-29*((y_b1(i)+yb0...
    -y_w1(i)-yw0)/40)],'g-','MarkerSize',5,'linewidth',3);
plot([-1+0.15,-1-0.15],[y_b1(i)+yb0-31*((y_b1(i)+yb0-y_w1(i)-yw0)/40),y_b1(i)+yb0-33*((y_b1(i)+yb0...
    -y_w1(i)-yw0)/40)],'g-','MarkerSize',5,'linewidth',3);
plot([-1+0.15,-1-0.15],[y_b1(i)+yb0-35*((y_b1(i)+yb0-y_w1(i)-yw0)/40),y_b1(i)+yb0-37*((y_b1(i)+yb0...
    -y_w1(i)-yw0)/40)],'g-','MarkerSize',5,'linewidth',3);
plot([-1+0.15,-1],[y_b1(i)+yb0-39*((y_b1(i)+yb0-y_w1(i)-yw0)/40),y_w1(i)+yw0],'g-','MarkerSize',5,...
    'linewidth',3);
%%%%%%%%%%
plot([-1, -1],[y_w1(i)+yw0, y_b1(i)+yb0],'b-','MarkerSize',5,'linewidth',10);
%%%%%%%%%%
plot([-1-0.15,-1+0.15],[y_b1(i)+yb0-((y_b1(i)+yb0-y_w1(i)-yw0)/40),y_b1(i)+yb0-3*((y_b1(i)+yb0...
    -y_w1(i)-yw0)/40)],'g-','MarkerSize',5,'linewidth',3);
plot([-1-0.15,-1+0.15],[y_b1(i)+yb0-5*((y_b1(i)+yb0-y_w1(i)-yw0)/40),y_b1(i)+yb0-7*((y_b1(i)+yb0...
    -y_w1(i)-yw0)/40)],'g-','MarkerSize',5,'linewidth',3);
plot([-1-0.15,-1+0.15],[y_b1(i)+yb0-9*((y_b1(i)+yb0-y_w1(i)-yw0)/40),y_b1(i)+yb0-11*((y_b1(i)+yb0...
    -y_w1(i)-yw0)/40)],'g-','MarkerSize',5,'linewidth',3);
plot([-1-0.15,-1+0.15],[y_b1(i)+yb0-13*((y_b1(i)+yb0-y_w1(i)-yw0)/40),y_b1(i)+yb0-15*((y_b1(i)+yb0...
    -y_w1(i)-yw0)/40)],'g-','MarkerSize',5,'linewidth',3);
plot([-1-0.15,-1+0.15],[y_b1(i)+yb0-17*((y_b1(i)+yb0-y_w1(i)-yw0)/40),y_b1(i)+yb0-19*((y_b1(i)+yb0...
    -y_w1(i)-yw0)/40)],'g-','MarkerSize',5,'linewidth',3);
plot([-1-0.15,-1+0.15],[y_b1(i)+yb0-21*((y_b1(i)+yb0-y_w1(i)-yw0)/40),y_b1(i)+yb0-23*((y_b1(i)+yb0...
    -y_w1(i)-yw0)/40)],'g-','MarkerSize',5,'linewidth',3);
plot([-1-0.15,-1+0.15],[y_b1(i)+yb0-25*((y_b1(i)+yb0-y_w1(i)-yw0)/40),y_b1(i)+yb0-27*((y_b1(i)+yb0...
    -y_w1(i)-yw0)/40)],'g-','MarkerSize',5,'linewidth',3);
plot([-1-0.15,-1+0.15],[y_b1(i)+yb0-29*((y_b1(i)+yb0-y_w1(i)-yw0)/40),y_b1(i)+yb0-31*((y_b1(i)+yb0...
    -y_w1(i)-yw0)/40)],'g-','MarkerSize',5,'linewidth',3);
plot([-1-0.15,-1+0.15],[y_b1(i)+yb0-33*((y_b1(i)+yb0-y_w1(i)-yw0)/40),y_b1(i)+yb0-35*((y_b1(i)+yb0...
    -y_w1(i)-yw0)/40)],'g-','MarkerSize',5,'linewidth',3);
plot([-1-0.15,-1+0.15],[y_b1(i)+yb0-37*((y_b1(i)+yb0-y_w1(i)-yw0)/40),y_b1(i)+yb0-39*((y_b1(i)+yb0...
    -y_w1(i)-yw0)/40)],'g-','MarkerSize',5,'linewidth',3);
%%% Draw tire
plot([-1,-1-0.08,-1+0.08,-1-0.08,-1+0.08,-1],[y_r(i)-0.381,y_r(i)-0.381-((y_r(i)-0.381-y_w1(i)+0.281)/8),...
    y_r(i)-0.381-3*((y_r(i)-0.381-y_w1(i)+0.281)/8),y_r(i)-0.381-5*((y_r(i)-0.381-y_w1(i)+0.281)/8),...
    y_r(i)-0.381-7*((y_r(i)-0.381-y_w1(i)+0.281)/8),y_w1(i)-0.281],'g-','MarkerSize',5,'linewidth',2);

%%%%%%%%%%%%%%%%%%%%%%%%%%%%%%%%%%%%%%%%%%%%%%%%%%%%%%%%%%%%%%%%%%%%%%%%%%%%%%%
%%%%%%%%%%             Proposed Active Suspension          %%%%%%%%%%%%%%%%
dxcy3=0.09;ycy03=1.5;dycy3=0.25; % Define Hydraulic Cylinder dimensions and initial position
dxs=-0.18;ys0=0.7;dys=0.1; % Define sprung mass dimensions
%%% Draw Car Body
x=[1+dxb, 1+dxb, 1-dxb, 1-dxb];
y=[y_b3(i)+yb0+dyb, y_b3(i)+yb0-dyb, y_b3(i)+yb0-dyb, y_b3(i)+yb0+dyb];
patch(x,y,'r'); hold on;
%%% Draw Hydraulic Cylinder
x=[1+dxcy3, 1+dxcy3, 1-dxcy3, 1-dxcy3];
y=[y_cy3(i)+ycy03+dycy3, y_cy3(i)+ycy03-dycy3, y_cy3(i)+ycy03-dycy3, y_cy3(i)+ycy03+dycy3];
patch(x,y,'b+'); hold on;
%%% Draw sprung mass
x=[1+dxs, 1+dxs, 1-dxs, 1-dxs];
y=[y_s(i)+ys0+dys, y_s(i)+ys0-dys, y_s(i)+ys0-dys, y_s(i)+ys0+dys];
patch(x,y,'r')
%%% Draw Wheel
t = 0:pi/20:2*pi;
patch(0.43*sin(t)+1,0.43*cos(t)+y_w3(i),'k')
patch(0.281*sin(t)+1,0.281*cos(t)+y_w3(i),'w')
%%% Draw conventional Suspension Connecting Sprung mass to Wheel
plot([1,1-0.15],[y_s(i)+ys0,y_s(i)+ys0-((y_s(i)+ys0-y_w3(i)-yw0)/20)],'g-','MarkerSize',5,...
    'linewidth',3);
plot([1+0.15,1-0.15],[y_s(i)+ys0-3*((y_s(i)+ys0-y_w3(i)-yw0)/20),y_s(i)+ys0-5*((y_s(i)+ys0...
    -y_w3(i)-yw0)/20)],'g-','MarkerSize',5,'linewidth',3);
plot([1+0.15,1-0.15],[y_s(i)+ys0-7*((y_s(i)+ys0-y_w3(i)-yw0)/20),y_s(i)+ys0-9*((y_s(i)+ys0...
    -y_w3(i)-yw0)/20)],'g-','MarkerSize',5,'linewidth',3);
plot([1+0.15,1-0.15],[y_s(i)+ys0-11*((y_s(i)+ys0-y_w3(i)-yw0)/20),y_s(i)+ys0-13*((y_s(i)+ys0...
    -y_w3(i)-yw0)/20)],'g-','MarkerSize',5,'linewidth',3);
plot([1+0.15,1-0.15],[y_s(i)+ys0-15*((y_s(i)+ys0-y_w3(i)-yw0)/20),y_s(i)+ys0-17*((y_s(i)+ys0...
    -y_w3(i)-yw0)/20)],'g-','MarkerSize',5,'linewidth',3);
plot([1+0.15,1],[y_s(i)+ys0-19*((y_s(i)+ys0-y_w3(i)-yw0)/20),y_w3(i)+yw0],'g-','MarkerSize',5,...
    'linewidth',3);
%%%%%%%%%%
plot([1, 1],[y_w3(i)+yw0, y_s(i)+ys0],'b-','MarkerSize',5,'linewidth',10);
%%%%%%%%%%
plot([1-0.15,1+0.15],[y_s(i)+ys0-((y_s(i)+ys0-y_w3(i)-yw0)/20),y_s(i)+ys0-3*((y_s(i)+ys0...
    -y_w3(i)-yw0)/20)],'g-','MarkerSize',5,'linewidth',3);
plot([1-0.15,1+0.15],[y_s(i)+ys0-5*((y_s(i)+ys0-y_w3(i)-yw0)/20),y_s(i)+ys0-7*((y_s(i)+ys0...
    -y_w3(i)-yw0)/20)],'g-','MarkerSize',5,'linewidth',3);
plot([1-0.15,1+0.15],[y_s(i)+ys0-9*((y_s(i)+ys0-y_w3(i)-yw0)/20),y_s(i)+ys0-11*((y_s(i)+ys0...
    -y_w3(i)-yw0)/20)],'g-','MarkerSize',5,'linewidth',3);
```

```
plot([1-0.15,1+0.15],[y_s(i)+ys0-13*((y_s(i)+ys0-y_w3(i)-yw0)/20),y_s(i)+ys0-15*((y_s(i)+ys0...
    -y_w3(i)-yw0)/20)],'g-','MarkerSize',5,'linewidth',3);
plot([1-0.15,1+0.15],[y_s(i)+ys0-17*((y_s(i)+ys0-y_w3(i)-yw0)/20),y_s(i)+ys0-19*((y_s(i)+ys0...
    -y_w3(i)-yw0)/20)],'g-','MarkerSize',5,'linewidth',3);
%%% Draw Hydraulic Cylinder rod Connecting Body/Chassis to Sprung mass
plot([1, 1],[y_s(i)+ys0+dys,y_b3(i)+yb0-dyb],'b-','MarkerSize',5,'linewidth',10);
%%% Draw tire spring
plot([1,1-0.08,1+0.08,1-0.08,1+0.08,1],[y_r(i)-0.381,y_r(i)-0.381-((y_r(i)-0.381-y_w3(i)+0.281)/8),...
    y_r(i)-0.381-3*((y_r(i)-0.381-y_w3(i)+0.281)/8),y_r(i)-0.381-5*((y_r(i)-0.381-y_w3(i)+0.281)/8),...
    y_r(i)-0.381-7*((y_r(i)-0.381-y_w3(i)+0.281)/8),y_w3(i)-0.281],'g-','MarkerSize',5,'linewidth',2);
%%%%%%%%%%%%%%%%%%%%%%%%%%%%%%%%%%%%%%%%%%%%%%%%%%%%%%%%%%%%%%%%%%%%%%%%%%%%
%%%%%%%%%%%%%%%%%%%%%%%%%%%%%%%%%%%%%%%%%%%%%%%%%%%%%%%%%%%%%%%%%%%%%%%%%%%%
%%% Draw Road
x=[-2, -2, 2, 2];
y=[-1, y_r(i)-0.381, y_r(i)-0.381, -1];
patch(x,y,'k')
%%% Label Figure
title('Response of Quarter-car Model with Active Suspension System')
xlabel('Ground')
ylabel('Vertical Position [m]')
%%% Scale Plot Axes
set(gca,'ylim',[-0.8,2.5])
set(gca,'xlim',[-0.2,0.2])
axis equal
grid on
end
hold off
```